4-aminoquinolines block heme iron reactivity and interfere with artemisinin action

Melissa R. Rosenthal[1], Daniel E. Goldberg[1,2*]

[1]Division of Infectious Diseases, Washington University School of Medicine, Saint Louis, MO United States of America.

[2]Department of Molecular Microbiology, Washington University School of Medicine, Saint Louis, MO United States of America.

*corresponding author: dgoldberg@wustl.edu

Abstract

Artemisinin-based combination therapies (ACTs) remain the mainstay of treatment for *Plasmodium falciparum* malaria, despite reports of ACT treatment failure. ACTs consist of an artemisinin and a longer-lived partner drug, which is often a quinoline. Given that heme is central to the mechanism of action of artemisinins and some quinolines, we hypothesized that these antimalarials would exhibit strong drug-drug interactions. Previous studies using standard 48 h or 72 h assays identified additive to mildly antagonistic interactions between artemisinins and quinolines. Here, we sought to re-evaluate these interactions using a pulsing assay that better mimics the short in vivo half-life of artemisinins. We found that chloroquine (CQ), piperaquine (PPQ), and amodiaquine substantially antagonize dihydroartemisinin (DHA), the active metabolite of artemisinins. CQ-DHA antagonism was notably exacerbated in CQ-resistant parasites, resulting in a superantagonistic phenotype in isobolograms. Further, we found that CQ co-treatment conferred artemisinin resistance to Kelch 13 wild type parasites in the ring stage survival assay. Using a small molecule probe to measure chemically reactive heme in live parasites, we determined that quinolines block artemisinin activation by rendering cytosolic heme inert. Finally, we probed beyond traditional ACTs, evaluating interactions of the proposed triple ACT, DHA-PPQ-Mefloquine, as well as OZ439-quinoline combinations, which were all found to be antagonistic. Collectively, these in vitro data suggest that peroxide-quinolines may have liabilities as combination therapies.

Introduction

Malaria was responsible for an estimated 263 million cases and 597,000 deaths in 2023, the majority of which were caused by *Plasmodium falciparum* [1]. The World Health Organization recommends artemisinin-based combination therapies (ACTs) for the treatment of *P. falciparum* malaria. ACTs are composed of a short-lived artemisinin derivative paired with a longer-lived partner drug. Depending on geographical resistance profiles, one of six combinations is recommended: Dihydroartemisinin (DHA) + Piperaquine (PPQ), Artesunate (AS) + Mefloquine (MFQ), AS + Amodiaquine (ADQ), AS + Pyronaridine (PYR), Artemether (AM) + Lumefantrine (LF), or AS + Sulfadoxine-pyrimethamine (SP). Three of these six partner drugs, PPQ, MFQ, and ADQ, possess quinoline groups. Importantly, heme is central to the mechanism of action of both artemisinins and quinolines [2,3].

Asexual blood stage parasites are adept at thriving in an incredibly heme rich environment. Parasites import up to 80% of host cell hemoglobin [4], which is transported to a specialized lysosome-like organelle, termed the digestive vacuole. Here, hemoglobin is proteolytically processed into globin peptides and redox active heme (Fe^{2+}-ferroprotoporphyrin IX), which is oxidized to hemin (Fe^{3+}-ferroprotoporphyrin IX) [5]. The majority of hemin is retained within the digestive vacuole where it is detoxified via sequestration into inert hemozoin crystals [6-8]. Hemin concentrations approach 0.5 M within the digestive vacuole [9]. Blood stage parasites also maintain a relatively high cytosolic heme concentration of approximately 1.6 μM [10]. While the source of this labile heme pool has not been experimentally determined, it is thought to originate from hemoglobin digestion.

The heme-rich environment of asexual blood stages has long been exploited for antimalarial intervention. The 4-aminoquinolines chloroquine (CQ) and PPQ are thought to act primarily in the parasite digestive vacuole, where they inhibit hemozoin formation by binding heme/hemin and the growing face of hemozoin [11-16]. It has been proposed that disruption of heme homeostasis and/or accumulation of toxic heme-quinoline complexes may contribute to parasite killing [17-19]. Resistance to 4-aminoquinolines is mediated by a collection of mutations in the chloroquine resistance transporter (PfCRT), which is located on the parasite digestive vacuole membrane [20]. Mutations in PfCRT are thought to mediate resistance by enabling drug efflux out of the digestive vacuole [2,21-24].

Heme is also central to the mechanism of action of artemisinins. Artemisinins contain a peroxide bridge that must be cleaved by heme for antimalarial activity [25-29]. Following activation, artemisinins non-specifically alkylate adjacent molecules, causing widespread cellular damage to the parasite [30-32]. Clinically, artemisinin resistance is primarily associated with mutations in Kelch 13 (K13) [33-35], which are thought to reduce parasite hemoglobin uptake and digestion [36-38]. Consequently, less heme is available to activate artemisinins.

ACTs remain the mainstay treatment for *falciparum* malaria. Widespread resistance to artemisinins in Southeast Asia and recent emergence of artemisinin resistance in Africa have posed great concern [1,34,39-42]. Reduced artemisinin efficacy means that the partner drugs are responsible for clearing a larger parasite biomass, increasing the likelihood for resistance to emerge to partner drugs. Indeed, high treatment failure rates have been reported for AS-MFQ, DHA-PPQ, and AS-ADQ in Southeast Asia [43-51].

Given that heme is central to the mechanism of action of both quinolines and artemisinins, we hypothesized that these antimalarials would exhibit strong drug-drug interactions. Previously, several groups have assessed quinoline-artemisinin interactions using standard 48 or 72 h assays

and found that combinations were additive in CQ-sensitive parasites and additive to slightly antagonistic in CQ-resistant parasites [52-56]. However, standard 48 h or 72 h assays in which parasites are exposed to compounds for the entire assay duration do not well represent clinical drug exposure conditions and can mask not only resistance phenotypes, but also drug-drug interaction phenotypes [57-60]. We sought to re-evaluate quinoline-artemisinin interactions in multidrug-sensitive, CQ-resistant, artemisinin-resistant, and PPQ-resistant parasites using pulsing assays that better represent artemisinin kinetics. Our work identifies that CQ, PPQ, and ADQ antagonize dihydroartemisinin (DHA), the active metabolite of clinically used artemisinins, likely by rendering heme chemically inert and preventing DHA activation. In addition, we explore drug-drug interactions beyond traditional ACTs, investigating interactions of putative triple ACTs as well as ozonide-quinoline combinations that failed in clinical trials. Overall, the data presented here highlight the importance of detailed investigation of drug-drug interactions, particularly in drug-resistant parasites.

Results

CQ and DHA are superantagonistic in CQ-resistant parasites

We began by evaluating CQ-DHA interactions in 3D7, a CQ-sensitive parasite, and Dd2, a CQ-resistant parasite (**Table 1**), using trophozoite-stage isobologram assays. Synchronized trophozoites were treated with fixed ratios of CQ and DHA for 4 h, drugs were washed off, and then parasitemia was assessed 72 h later. Given the short half-life of artemisinins [58], we believe that this pulsing format allows us to better assess the effect of ACT partner drugs on DHA activity compared to standard 48 or 72 h assays. Fractional IC50 (FIC50) values were calculated from fixed ratios and then plotted on an XY-graph to generate isobolograms. Isobolograms can be interpreted based on isobole shape and mean ΣFIC50 values as follows: points along the dotted line with a mean ΣFIC50 value close to 1 indicate additivity, points above the dotted line in a concave curve with a mean ΣFIC50 value >1.25 indicate antagonism, and points below the dotted line in a convex curve with a mean ΣFIC50 value <0.75 indicate synergy.

We observed strong antagonism for CQ-DHA in 3D7 parasites (**Figure 1a**), with a mean ΣFIC50 value of 1.68. Antagonism was notably exacerbated in Dd2 parasites (**Figure 1b**), which had a mean ΣFIC50 value of 2.44. The magnitude of this value far surpasses conventional antagonism, and we termed this phenomenon “superantagonism”. Perhaps even more unexpected was the atypical shape of this isobole (**Figure 1b**), where points extended upward and peak ΣFIC50 values exceeded 4. In contrast, peak ΣFIC50 values for 3D7 reached only 2.

The traditional isobole shape for 3D7 indicates a reciprocal relationship between CQ and DHA, whereas the atypical isobole shape of Dd2 suggests a one-sided relationship, whereby CQ is blocking DHA activity.

Multiple groups have demonstrated that parasite genetics can influence drug-drug interactions [55,61,62]. 3D7 and Dd2 parasites differ genetically at a number of drug resistance markers, including PfCRT which is responsible for mediating CQ resistance. To determine if PfCRT genotype was responsible for differences in CQ-DHA interactions between these parasite lines, we evaluated interactions in two Dd2 parasites that are isogenic except at PfCRT [63,64]: Dd2 PfCRT^{3D7}, which is edited to have the 3D7 PfCRT genotype, and Dd2 PfCRT^{Dd2}, which maintains the Dd2 PfCRT genotype and was used as a cloning control (**Table 1**). Notably, superantagonism was lost in Dd2 PfCRT^{3D7} parasites, which phenocopied 3D7 parasites, and had a mean ΣFIC50 value of 1.85 and a conventional isobole shape (**Figure 1c**). In contrast, Dd2 PfCRT^{Dd2} parasites displayed one-sided superantagonism with a mean ΣFIC50 value of 2.73 and peak ΣFIC50 values > 4.5 (**Figure 1d**). These data suggest that PfCRT genotype is the main genetic determinant that dictates CQ-DHA interactions.

Both 3D7 and Dd2 parasites are artemisinin sensitive, harboring a wildtype K13. To determine if resistance to artemisinins alters CQ-DHA interactions, we next evaluated CQ-DHA combinations in Dd2 parasites that are edited to have a K13^{R539T} mutation [35] (**Table 1**). Dd2 K13^{R539T} parasites, which also harbor a Dd2 PfCRT genotype, displayed a one-sided superantagonistic isobole that was reminiscent of both Dd2 and Dd2 PfCRT^{Dd2} parasites (**Figure 1e**). This suggests that, unlike PfCRT genotype, K13 genotype appeared to have no impact on drug-drug interactions at the trophozoite stage.

PPQ and DHA are antagonistic

Next, we sought to evaluate drug-drug interactions of DHA and the ACT partner drugs PPQ and MFQ. PPQ is believed to have a similar mechanism of action as CQ and both antimalarials are 4-aminoquinolines. Accordingly, we hypothesized that PPQ and DHA would also be antagonistic. In 3D7, Dd2, Dd2 PfCRT^{3D7}, Dd2 PfCRT^{Dd2}, and Dd2 K13^{R539T} trophozoites, we observed conventional antagonism for PPQ-DHA (**Figure 1f-j**) with mean ΣFIC50 values ranging from 1.55 to 1.71. To determine if, similar to CQ, PPQ-DHA interactions would be exacerbated in PPQ-resistant parasites, we also evaluated Dd2 PfCRT^{M343L}, which harbors the Dd2 PfCRT plus an additional mutation at M343L [64] (**Table 1**). The M343L mutation had no impact on PPQ-DHA interactions and Dd2 PfCRT^{M343L} parasites displayed conventional antagonism with a mean ΣFIC50 value of 1.58 (**Figure 1k**). Note that while the PPQ IC50 of Dd2 PfCRT^{M343L} is 2.5-fold

higher than Dd2 (65 nM versus 25 nM; **Figure 1- figure supplement 1**), this shift is substantially smaller than the >1000-fold CQ IC50 shift that we and others [60] have observed in CQ-sensitive versus CQ-resistant parasites using the pulsing assay format (**Figure 1- figure supplement 1**).

Next, we assessed interactions between MFQ and DHA (**Figure 1l-q**). Though MFQ contains a quinoline group, it is chemically classified as an aryl amino alcohol and is believed to have a heme-independent mechanism of action [65]. Consistent with this, we observed additivity for MFQ-DHA in all six parasites tested with mean ΣFIC50 values ranging from 0.94 to 1.20. This additivity along with the synergism that we previously reported for DHA-proteasome inhibitor combinations [61], provides context for the antagonism and superantagonism that we observed for PPQ-DHA and CQ-DHA.

CQ combination treatment confers artemisinin resistance to K13^{WT} parasites in ring-stage survival assays

Given our observation that CQ and PPQ antagonize DHA in trophozoite stages, we next sought to determine if these quinolines would promote survival in early ring stages where artemisinin resistance is classically observed. We performed DHA dose-response assays on early ring stage parasites to determine both ring-stage survival assay (RSA) values and IC50 values (**Figure 2a and Figure 2- figure supplement 1**). The RSA is used to delineate artemisinin-sensitive versus resistant parasites, where survival > 1% corresponds to resistance and < 1% indicates sensitivity [58]. Though DHA IC50 values cannot reliably differentiate artemisinin sensitive vs resistant parasites [58], they can provide important insight into different factors that contribute to artemisinin susceptibility [66].

In the absence of quinolines, the artemisinin sensitive K13^{WT} parasites, Dd2 PfCRT^{3D7} and Dd2, had RSA survival values ≤ 1%, while Dd2 K13^{R539T} had an RSA survival of 12.63% (**Figure 2b-d *top panel***). Co-treatment with 10 μM CQ, a pharmacologically relevant concentration [67,68], significantly increased RSA survival, conferring artemisinin resistance to both Dd2 PfCRT^{3D7} and Dd2 parasites with mean RSA values of 2.66% and 4.49%, respectively (**Figure 2b and c *top panel***). RSA survival values were also increased in Dd2 K13^{R539T} parasites to 18.39%, although this shift was not statistically significant (**Figure 2d *top panel***). When assessing DHA sensitivity by ring-stage IC50 values, CQ co-treatment also had a substantial rescuing effect in both Dd2 and Dd2 K13^{R539T} parasites, resulting in a 4-fold increase in DHA IC50 (**Figure 2c and d *bottom panel***). Note that while we were unable to determine a DHA IC50 value for CQ-sensitive Dd2 PfCRT^{3D7} parasites in the presence of 10 μM CQ, the dose-response curve was suggestive of antagonism (**Figure 2- figure supplement 1a**).

To determine if PPQ would have a similar rescuing effect, we performed these same assays in the presence of 200 nM PPQ. This concentration was chosen because it is sublethal for early rings in this short 3 h pulse, pharmacologically relevant [69,70], and mimics the PPQ survival assay (PSA) that is used to delineate PPQ resistance [57]. Co-treatment with 200 nM PPQ did not have a rescuing effect for Dd2 PfCRT^{3D7}, Dd2, or Dd2 K13^{R539T} parasites and resulted in mean RSA values that were either similar to or lower than the DHA-only control (**Figure 2b-d**). Note that in the absence of DHA, 200 nM PPQ inhibited parasite growth approximately 20%. However, co-treatment with 200 nM PPQ did not shift the IC50 values or DHA dose response curves of these parasites (**Figure 2b-d and Figure 2- figure supplement 1a-c**), indicating that PPQ and DHA are also antagonistic in early ring stages.

We were curious if higher concentrations of PPQ might have a rescuing effect, particularly for PPQ-resistant parasites that are capable of surviving a higher PPQ dose. To this end, we assayed two PPQ-resistant parasites: Dd2 PfCRT^{M343L} and MRA-1284 (IPC_6261), which is an artemisinin-resistant and PPQ-resistant clinical isolate that was collected in 2012 from Cambodia (**Table 1**). Dd2 PfCRT^{M343L} and MRA-1284 have PPQ survival values (PSA) of 10% [64] and 40% [71], respectively. While co-treatment with 10 μM CQ had a rescuing effect for Dd2 PfCRT^{M343L} as assessed by RSA and IC50 values, neither 200 nM PPQ, 500 nM PPQ, or 10 μM PPQ co-treatment rescued parasite survival (**Figure 2e and Figure 2- figure supplement 1d**). Similarly, 10 μM CQ co-treatment decreased MRA-1284 sensitivity to DHA as assessed by RSA and early ring IC50 values, while co-treatment with 200 nM PPQ or 500 nM PPQ had no effect on DHA sensitivity (**Figure 2f**). This phenotype is consistent with conventional antagonism. Interestingly, while co-treatment with 10 μM PPQ did not alter the RSA survival of MRA-1284, it did shift the dose-response curve to the left (**Figure 2- figure supplement 1e**). However, since 10 μM PPQ inhibited parasite growth approximately 60% on its own, we were unable to determine an IC50 value.

CQ and PPQ interfere with heme iron reactivity

In total, we profiled three different quinoline-DHA interactions, which are summarized in **Figure 3a**. In solution, quinolines and heme form heme-quinoline complexes, wherein heme is present as a μ-oxo dimer [72-74]. Though the exact stoichiometry of this interaction for each quinoline remains debated [72-76], formation of such a complex could render quinoline-bound heme chemically inert (i.e. unable to activate artemisinins).

To investigate this, we utilized a recently developed small molecule probe, H-FluNox, that is highly sensitive and specific for heme over hemin, heme-bound proteins, Fe^{2+}, and other salts

and metal ions [77]. H-FluNox is basally non-fluorescent, but upon cleavage of a N-O bond by the Fe^{2+} of heme, H-FluNox fluoresces [77] (**Figure 3b *top panel***). While not identical, this reaction is similar to artemisinin activation, which requires cleavage of artemisinin's peroxide bond by the Fe^{2+} of heme [29] (**Figure 3b *bottom panel***). To determine if quinoline-heme complexes would react with H-FluNox, we began by assessing H-FluNox fluorescence in solution with 10 μM CQ, which is sub-lethal for CQ-resistant parasites and pharmacologically relevant [67,68]. Relative to the untreated control, 10 μM CQ inhibited fluorescence approximately 50% in the presence of 250 nM heme (**Figure 3c**). This suggests that heme iron reactivity is impaired when heme is in complex with CQ. Next, we evaluated PPQ and MFQ at two different concentrations: 150 nM, which reflects a 5x trophozoite-stage IC50 concentration, and 10 μM to directly compare these quinolines with CQ. At 150 nM, both PPQ and MFQ inhibited fluorescence, albeit only 10% (**Figure 3c**). At 10 μM, MFQ inhibited fluorescence to a similar extent as CQ, while 10 μM PPQ only inhibited fluorescence 25% (**Figure 3c**). Note that 10 μM concentrations exceed maximum plasma concentrations of PPQ and MFQ, which have been reported to reach approximately 0.5-1 μM and 5 μM, respectively [69,70,78].

Next, we assessed fluorescence in live trophozoite stage parasites using the cell permeable analog of H-FluNox, Ac-H-FluNox [77]. In untreated Dd2 parasites, fluorescence was predominantly observed in the parasite cytoplasm (**Figure 3d**), and little signal was detected in red blood cells or the parasite digestive vacuole. This suggests that a significant portion of DHA could be activated in the parasite cytoplasm. Lack of signal in the digestive vacuole could be due to issues with permeability, the specificity of Ac-H-FluNox for heme over hemin (the predominant heme species in the digestive vacuole), or sensitivity of Ac-H-FluNox to a low pH environment. In solution, H-FluNox fluorescence was decreased approximately 60% at pH 5.4 (**Figure 3- figure supplement 1a**), which is the estimated pH of the digestive vacuole [79]. However, alkalinization of the digestive vacuole with ammonium chloride [80] did not increase digestive vacuole fluorescence signal (**Figure 3- figure supplement 1b**), suggesting that low pH alone cannot explain this lack of labeling.

Importantly, treatment of Dd2 trophozoites with 10 μM CQ nearly ablated Ac-H-FluNox fluorescent signal (**Figure 3d and e**). Treatment with 150 nM PPQ also significantly reduced fluorescence, though not to the same extent as 10 μM CQ (50% inhibition versus > 92% inhibition) (**Figure 3d, e, and Figure 3 and 4- table supplement 1**). In contrast, parasites treated with 150 nM MFQ had similar fluorescence as untreated control parasites (**Figure 3d and e**). These assays with H-FluNox and Ac-H-FluNox correlate well with hemozoin inhibition assays in which CQ, PPQ, and MFQ inhibit hemozoin formation in solution [73], but only CQ and PPQ inhibit hemozoin

formation in parasites [7,81-83]. To determine if concentration alone was responsible for the differences that we observed between CQ and the other quinolines, we also evaluated Ac-H-FluNox fluorescence following treatment with 10 μM PPQ or 10 μM MFQ. At this super-physiological and super-lethal concentration, an equimolar concentration of CQ still inhibited H-FluNox fluorescence to a greater extent than PPQ or MFQ (**Figure 3- figure supplement 2 and Figure 3 and 4- table supplement 1**). This suggests that something unique to the chemistry of CQ and/or the biology of the parasite is responsible for the differences that we observed.

PfCRT^{Dd2} is believed to mediate CQ resistance by pumping CQ out of the digestive vacuole [2,21-24], suggesting that cytoplasmic CQ concentrations may differ between PfCRT^{Dd2} and PfCRT^{3D7} parasites treated with the same concentration of CQ. Given the substantial difference that we saw in the shape of CQ-DHA isobolograms between PfCRT^{Dd2} and PfCRT^{3D7} parasites, we were curious if differences in PfCRT genotype would impact Ac-H-FluNox fluorescence. Accordingly, we treated Dd2 PfCRT^{Dd2} and Dd2 PfCRT^{3D7} parasites with 150 nM CQ or 10 μM CQ and measured chemically "reactive" heme using Ac-H-FluNox. In untreated Dd2 PfCRT^{Dd2} versus Dd2 PfCRT^{3D7} parasites, we observed no difference in Ac-H-FluNox localization or fluorescence intensity (**Figure 3f and Figure 3- figure supplement 3**). Following treatment with 150 nM CQ, fluorescence was inhibited 25% in Dd2 PfCRT^{3D7} and 35% in Dd2 PfCRT^{Dd2}, although this difference was not statistically significant (**Figure 3f and Figure 3 and 4- table supplement 1**). Curiously, while 10 μM CQ treatment reduced mean fluorescence approximately 60% in Dd2 PfCRT^{3D7} parasites, it was not to the extent of Dd2 PfCRT^{Dd2} parasites (80%) (**Figure 3f and Figure 3 and 4- table supplement 1**). These data suggest that transport of CQ out of the digestive vacuole by PfCRT^{Dd2} may contribute to superantagonism between CQ and DHA in CQ-resistant parasites.

CQ co-treatment rescues DHA-mediated protein damage

Following activation by heme, DHA causes widespread protein damage in the parasite [30-32,84]. Accordingly, we would expect that if CQ is antagonizing DHA activation, then CQ co-treatment should rescue DHA-mediated protein damage. To test this hypothesis, we treated Dd2 trophozoites with CQ, DHA, or CQ + DHA and probed for K48-linked ubiquitin, which is a marker of protein damage [84]. Consistent with what has been previously reported [85], CQ treatment alone had no effect on K48-linked ubiquitin levels, while treatment with DHA resulted in a 2-fold increase in K48-linked ubiquitin (**Figure 3g, h, and Figure 3- figure supplement 4**). Importantly, addition of CQ to DHA had a rescuing effect, resulting in levels of K48-linked ubiquitin that were similar to the DMSO-treated control (**Figure 3g and h**). Collectively, these data suggest that CQ

antagonizes DHA by rendering heme chemically inert, reducing DHA activation, and consequently, reducing DHA-mediated protein damage.

PPQ and MFQ do not harm treatment efficacy, but strongly antagonize each other.

With the looming threat of widespread ACT treatment failure, several ideas have been proposed to delay the spread of ACT resistance by using currently available antimalarials. Triple ACTs (TACTs), which are composed of a traditional ACT plus an additional longer-lived partner drug, have gained the most traction. Early clinical trials indicate that DHA-PPQ-MFQ and AM-LM-ADQ show good safety and efficacy against artemisinin-sensitive and resistant parasites [47,86-88]. We were curious how the addition of a third antimalarial would influence drug interactions. Accordingly, we performed trophozoite-stage DHA dose response assays on Dd2 parasites in the presence of a fixed, sub-lethal concentration of PPQ, MFQ, or PPQ + MFQ. Addition of 2 nM DHA was also included as a control to represent additivity. As assessed by DHA IC50 values, addition of 15 nM PPQ did not improve parasite killing, while addition of 15 nM MFQ resulted in a 3-fold decrease in IC50 compared to the DMSO control (**Figure 4a and b**). These phenotypes are consistent with antagonistic and additive relationships, respectively. Notably, addition of PPQ + MFQ had no additional benefit compared to addition of MFQ alone (**Figure 4 a and b**).

Following the initial 3-day TACT treatment regimen, long-lived partner drugs are responsible for clearing the remaining parasite burden. Accordingly, we sought to assess drug-drug interactions of PPQ-MFQ in the absence of DHA. Previously it was reported that MFQ and PPQ were moderately antagonistic in 3D7 and K1 parasites using a standard 48 h assay, with mean ΣFIC50 values of 1.31 and 1.28, respectively [52]. Using our trophozoite-stage assay, we observed reciprocal superantagonism in both PPQ-sensitive, Dd2 (**Figure 4c**), and PPQ-resistant Dd2 PfCRT^{M343L} (**Figure 4- figure supplement 1a**), with mean ΣFIC50 values of 2.62 and 2.44, respectively. This phenotype appears to be unique to PPQ, as we observed only strong antagonism for CQ-MFQ with a mean ΣFIC50 of 1.72 (**Figure 4- figure supplement 1b**). Overall, these in vitro data suggest that based on drug-drug interactions, PPQ and MFQ may not be a strategic long-lived antimalarial pairing for TACTs.

Quinolines antagonize peroxides

To determine if the drug-drug interactions that we evaluated were specific to a subset of antimalarials or represented a broader phenotype, we next evaluated DHA interactions with the clinically used ACT partner drugs ADQ and LM. Structurally, ADQ is classified as a 4-aminoquinoline like PPQ and CQ, while LM is classified as an aryl amino alcohol like MFQ.

However, unlike MFQ, LM lacks a quinoline group. We found that in Dd2 parasites, ADQ and DHA were antagonistic (**Figure 4d**) with a mean ΣFIC50 of 1.61, while LM and DHA were additive (**Figure 4e**) with a mean ΣFIC50 of 1.02.

To determine if 4-aminoquinolines antagonize other peroxide antimalarials, we next sought to assess interactions of two different OZ439-quinoline pairs that were previously evaluated in clinical trials. Similar to artemisinins, the synthetic ozonide, OZ439, requires activation via heme-mediated cleavage of a peroxide bond, but has a significantly improved half-life of 46-62 h [89]. In phase II clinical trials, OZ439 showed good efficacy alone [89], but poor efficacy either in combination with PPQ [90] or the next generation quinoline, ferroquine (FQ) [91,92]. To assess drug-drug interactions, we performed trophozoite-stage isobolograms with OZ439-PPQ and OZ439-FQ in Dd2 parasites. The pulsing format was used to maintain consistency across experiments. Both PPQ-OZ439 (**Figure 4f**) and FQ-OZ439 (**Figure 4g**) were antagonistic with mean ΣFIC50 values of 1.42 and 1.52, respectively. These data suggest that antagonistic interactions are potentially one of several factors [90-94] that may have contributed to the poor efficacy of these single dose combination therapies.

Although the mechanism of action of ADQ and FQ are less well studied, both antimalarials appear to inhibit hemozoin formation. ADQ was shown to inhibit hemozoin formation in parasites using the heme fractionation assay [83]. While in-parasite assays have not been performed with FQ, in vitro biochemical studies suggest that FQ may inhibit hemozoin formation even better than CQ [95]. Accordingly, we were curious if ADQ and FQ treatment would “inactivate” heme in parasites. Using the Ac-H-FluNox heme probe, we observed that relative to the untreated control, treatment with 150 nM ADQ or 150 nM FQ (approximate 5x IC50 concentrations; **Figure 4- figure supplement 2**) reduced Ac-H-FluNox fluorescent signal approximately 50% and 55%, respectively (**Figure 4h, i, and Figure 3 and 4- table supplement 1**). In contrast, treatment with an equipotent concentration of LM had no significant impact on Ac-H-FluNox signal relative to the untreated control (**Figure 4h and i**). Among the six partner drugs that were evaluated, we observed a clear inverse correlation between Ac-H-FluNox signal and mean ΣFIC50, with an R^2 value of 0.84 (**Figure 4j**). These data strongly suggest that antimalarials that render heme inert also antagonize artemisinin and ozonide antimalarials, presumably by blocking endoperoxide activation.

Discussion

Combination therapies are widely believed to delay the emergence of drug resistance not only for malaria, but also bacterial infections, HIV, fungal infections, and cancer. However, to

maximize the benefits of combination therapies, it is essential that drugs are strategically paired. At a minimum, combinations should enhance efficacy to reduce parasite biomass and reduce the potential for drug resistance to evolve. In vitro assessment of drug-drug interactions between two antimalarials with vastly different half-lives is challenging. We chose to use a short treatment pulse to mimic artemisinin exposure and gain an understanding into how quinolines impact artemisinin activity. While drug-drug interactions are undoubtably much more complex in vivo, we believe this assay format better recapitulates clinical conditions compared to traditional 48 or 72 h assays.

We found that CQ and PPQ are antagonistic with DHA as assessed in early ring and trophozoite stages across three different parasite backgrounds. Artemisinin resistance is thought to be mediated by reduced heme-mediated activation and/or enhanced parasite stress response. Accordingly, 4-aminoquinolines could antagonize DHA by either or both mechanism(s). Our work with Ac-H-FluNox suggests that 4-aminoquinolines antagonize DHA by rendering intra-parasitic heme chemically inert, thus blocking DHA activation. However, future work will be needed to assess the effect of 4-aminoquinolines on parasite stress responses.

To date, it remains debated where artemisinins are activated within the parasite. There are several lines of evidences that suggest that artemisinins can be activated in the parasite cytoplasm. First, immunofluorescence studies with an anti-AS antibody [96] and live cell imaging with an artemisinin-based photoaffinity probe [97] revealed that artemisinins localize throughout the parasite cytoplasm. Second, numerous chemical proteomics studies utilizing artemisinin and ozonide-based click chemistry probes have identified a number of cytoplasmic proteins as targets of artemisinin and ozonides [30-32,98,99]. Given how quickly activated artemisinins react with adjacent molecules, it is unlikely that activated artemisinins could traverse the digestive vacuole or other organelle membranes before encountering a cytoplasmic target. Finally, immunofluorescence assays with antibodies specific for the alkylation signature of the ozonide OZ277 [100] revealed labeling throughout the parasite cytoplasm. Our data with Ac-H-FluNox also lend credence to this hypothesis. We observed Ac-H-FluNox fluorescence throughout the parasite cytoplasm, indicating that there is a substantial amount of heme in this location that is chemically competent to activate artemisinins. It is possible that technical limitations, such as issues with membrane permeability, limit Ac-H-FluNox fluorescence in the digestive vacuole. Nevertheless, these data collectively indicate that artemisinins can be activated in the parasite cytoplasm.

Previously, it has been reported that CQ treatment increases intracellular “free” heme [7,10,101]. However, the term “free” heme is somewhat malleable. While the pyridine-heme fractionation assay [7,83], electron spectroscopic imaging (ESI) with energy-loss spectroscopy (EELS) [7] and heme biosensor [10], can be used to detect and quantify heme species, they are

unable to differentiate chemically “active” heme from inert heme (i.e. quinoline bound or protein bound). In contrast, H-FluNox is highly specific for chemically “active” heme [77]. One possibility to reconcile our data with previous reports is that CQ treatment increases non-hemozoin/hemoglobin heme, but that this heme is bound to CQ or other biomolecules, rendering it unable to activate Ac-H-FluNox or peroxides. It is important to note that the chemistry of artemisinin and Ac-H-FluNox activation are not identical and these data with Ac-H-FluNox should be interpreted with caution. Nevertheless, we believe that Ac-H-FluNox is the best currently available proxy to assess artemisinin activation in live parasites.

CQ-DHA antagonism was notably exacerbated in CQ-resistant parasites. The concentrations used in isobolograms are chosen based on parasite IC50 values to individual compounds. While all parasites were exposed to similar DHA concentrations, CQ-resistant parasites were exposed to much higher CQ concentrations compared to their CQ-sensitive counterparts. This may explain in part why antagonism was intensified in CQ resistant parasites. However, equimolar treatment with 10 μM CQ resulted in significantly lower Ac-H-FluNox signal in Dd2 PfCRT^{Dd2} versus Dd2 PfCRT^{3D7} parasites (**Figure 3f**). These data could suggest that while the majority of CQ is sequestered in the digestive vacuole of Dd2 PfCRT^{3D7} parasites, PfCRT^{Dd2} is able to transport more CQ out of the digestive vacuole, thus allowing more CQ to bind cytosolic heme in parasites harboring a PfCRT^{Dd2}. This duality of PfCRT^{Dd2}, simultaneously enhancing parasite survival to CQ while promoting cytoplasmic heme “inactivation”, may explain the unprecedented one-sided superantagonistic isobole that we observed.

Fortunately, we did not observe superantagonism with DHA-PPQ in PPQ-resistant parasites. With a modest 3-fold shift in PPQ IC50 between Dd2 vs Dd2 PfCRT^{M343L} parasites (25 nM vs 65 nM), it is perhaps unsurprising that no significant difference in DHA-PPQ isobolograms was observed between these two parasites. This is in contrast to the >1000-fold CQ IC50 shift that we and others [60] have observed between CQ-sensitive and CQ-resistant parasites using pulsing assays. Our studies with Ac-H-FluNox indicate that 150 nM PPQ is sufficient to render approximately 50% of available heme inert (**Figure 3e**). While these data suggest that PPQ blocks some DHA activation, it is likely that 150 nM PPQ is not sufficient to block all DHA activation. Since even PPQ-resistant parasites are at least partially susceptible to mid-nanomolar PPQ concentrations, the protective effect that PPQ has in neutralizing DHA is partially negated by PPQ-mediated killing. In contrast, CQ-resistant parasites are relatively unaffected by pulses with low micromolar CQ concentrations. Accordingly, CQ concentrations that are high enough to nearly block all DHA activation are insufficient to kill CQ resistant parasites.

Relative to PPQ and MFQ, CQ appears to have the greatest ability to impair heme iron reactivity. We were surprised to observe that PPQ inhibited H-FluNox fluorescence only half as well as CQ in solution. This suggests that there may be important differences in how these 4-aminoquinolines bind heme. In Dd2 parasites, CQ also inhibited Ac-H-FluNox fluorescence to a greater extent than PPQ at 10 μM concentrations. Given that the ability of CQ to "inactivate" heme in parasites is dependent on PfCRT genotype, it is possible that these results may differ in a PPQ-resistant parasite. In solution, equimolar concentrations of CQ and MFQ inhibited H-FluNox fluorescence to a similar extent, while MFQ had a minimal effect on Ac-H-FluNox fluorescence at even super-pharmacological concentrations. This was somewhat surprising given that MFQ is believed to act in the parasite cytoplasm [102,103]. It possible that differences in how MFQ binds to heme [73], affinity of MFQ for other biomolecules [104], and/or modification of MFQ within the parasite could contribute to this discrepancy.

In the early 2000's, the rise of CQ resistance prompted a search for new combination therapies [105]. Several clinical trials were conducted in West Africa to compare efficacy of CQ versus CQ-AS. On day 28, two studies reported similar failure rates for CQ and CQ-AS [106,107]. In in a third study, cure rates were significantly higher for CQ-AS compared to CQ alone [108]. However, all three studies recommended against use of CQ-AS, due to poor treatment efficacy. Notably, AS-SP and AS-LM were reported to show > 97% efficacy on West African populations during the same time period [109,110]. In contrast to superantagonism, in vitro conventional antagonism does not appear to correlate well with treatment failure. ACTs, including DHA-PPQ and AS-ADQ, are highly effective, provided that parasites remain sensitive to one or both ACT component(s). It has yet to be evaluated if antagonistic combinations have silent consequences that might discourage their clinical implementation. For example, since PPQ and ADQ appear to block artemisinin activation, it is possible that these combinations are acting more like pseudo-monotherapies than true combination therapies. This could have a number of downstream consequences, such as impacting the rate of drug resistance evolution. However, future work is needed to address these concerns.

With the absence of new antimalarials ready for clinical implementation, novel strategies with existing drugs have been proposed to overcome current problems with ACT treatment failures. One such strategy, TACTs, has gained the most traction. For traditional ACTs, the short one hour half-life of artemisinins means that long-lived partner drugs are essentially acting as monotherapies for most of the initial 3-day treatment regimen and a substantial period thereafter. In the case of artemisinin-resistant parasites, partner drugs must clear a significantly higher parasite biomass, which increases the likelihood for resistance to emerge. In theory, TACTs are

designed to overcome this flaw, whereby two partner drugs with similar half-lives are used, ensuring that parasites are always exposed to at least two antimalarials [111,112]. In clinical trials, DHA-PPQ-MFQ showed improved efficacy over DHA-PPQ in regions of high PPQ-resistance [47]. However, some have speculated that this was solely due to application of MFQ to MFQ-sensitive parasites and that the TACT would be no more effective than DHA-MFQ [113]. PPQ and MFQ were initially promoted as ideal partner drugs for TACTs as it was thought that either due to collateral sensitivity or fitness costs, dual PPQ and MFQ resistance was unlikely to occur [114,115]. Use of edited isogenic lines suggests that PPQ resistance conferring mutations in PfCRT have no effect on MFQ sensitivity, while increased MDR1 copy number, which underlies MFQ-resistance, has no effect on PPQ sensitivity [81]. Further, more recent genetic surveillance studies of Cambodian parasites cast doubt on the hypothesis that a DHA-PPQ-MFQ resistant parasite would be unfit to spread clinically [116]. Previous reports using standard 48 or 72 h assays indicated that PPQ and MFQ are modestly antagonistic [52,55]. Interestingly, we observed a much more pronounced superantagonistic phenotype using a pulsing format. It is important to note that unlike artemisinins, PPQ and MFQ have half-lives of several weeks [117,118], raising the question of which assay format would be best suited to evaluate interactions of long-lived partner drugs. Nevertheless, given the interplay of existing PPQ-resistance and PPQ-MFQ antagonism, MFQ and PPQ should, perhaps, be further scrutinized as potential partners for TACTs.

The synthetic ozonide, OZ439, was previously poised to replace artemisinins in combination therapies. While OZ439 is believed to have a mechanism of action similar to that of artemisinins, it has a notably improved 46-62 h half-life [89] and was shown to be effective against artemisinin-resistant parasites [119-121]. While OZ439 showed good efficacy alone [89], high treatment failure as part of single-dose combination therapies ultimately resulted in loss of interest of this antimalarial [90-92]. However, our data suggest that unsuitable choices in partner drugs may be one of several factors, including poor drug exposure [90-92] and preexisting PPQ-resistance [93,94], that contributed to the poor therapeutic efficacy of these combinations. As assessed by Ac-H-FluNox, both PPQ and FQ appear to rendered heme inert, thus blocking OZ439 activation. Biochemical studies have predicted that due to its less basic behavior, FQ might have a lower propensity to accumulate in the parasite digestive vacuole compared to CQ [95]. Greater accumulation of FQ in the parasite cytoplasm compared to other quinolines might explain the ability of FQ to greatly diminish Ac-H-FluNox signal even at nanomolar concentrations. Clinically, peak levels of FQ have been reported to reach approximately 0.5 μM [122], which could significantly impact OZ439 activation. However, unlike CQ, mid-nanomolar FQ concentrations are lethal for parasites, which may explain why we did not observe a super antagonistic phenotype for FQ-OZ439.

The antimalarials that we have are a precious resource, and it is only a matter of time before they fail. Our work clearly demonstrates the importance of detailed understanding of drug-drug interactions at the parasite level. While we believe the pulsing assay used in this study better mimics artemisinin pharmacokinetics compared to standard 72 h assays, it is not suitable for high throughput format. Recently, a high throughput assay was developed to evaluate drug-drug and drug-drug-drug interactions in *P. falciparum* [55]. Using this assay, the authors were able to evaluate interactions of 16 potential TACT combinations against 13 clinical isolates [55]. Similar to our findings, the authors reported that interactions can be highly dependent on parasite genetics. This high throughput assay will undoubtably be an important first step in evaluating interactions of new combinations. Nevertheless, since this assay relies on a 72 h format, additive interactions should be interpreted with caution, as this format can mask drug-drug interactions [59]. Accordingly, pulsing assays like the one used in this study will be an important step for investigating drug-drug interactions, prior to in vivo studies [123].

Materials and Methods

Reagents. All reagents were purchased from Sigma-Aldrich unless otherwise indicated.

Parasite Culture. Dd2 PfCRT^{Dd2}, Dd2PfCRT^{3D7}, Dd2 PfCRT^{M343L}, and Dd2 K13^{R539T} were kindly provided by Dr. David Fidock (Columbia University) [35,64]. MRA-1284 was obtained through BEI Resources, NIAID, NIH: *Plasmodium falciparum*, Strain IPC_6261, MRA-1284, contributed by Didier Ménard. Parasites were propagated in human red blood cells obtained from St. Louis Children's Hospital blood bank. Cultures were grown at 5% hematocrit in media containing RPMI1640 (Gibco) supplemented with 0.25% (wt/vol) Albumax (Gibco), 15 mg/L hypoxanthine, 110 mg/L sodium pyruvate, 1.19 g/L HEPES, 2.52 g/L sodium bicarbonate, 2 g/L glucose, and 10 mg/L gentamicin and were maintained in air-tight chambers filled with 5% O_2/5%CO_2/90%N_2 at 37°C.

Trophozoite-Stage Dose-Response Assays and Isobolograms. Trophozoite-stage assays were performed as previously described with minor modifications [61]. Briefly, parasites were synchronized to the trophozoites stage using two consecutive treatments with 5% sorbitol 10 h apart, followed by culturing for an additional 14 h. Trophozoite stages were seeded at 0.2% parasitemia and 1% hematocrit in round-bottom 96-well plates. Following 4 h incubation with antimalarials, infected red blood cells were washed a minimum of 5 times for plates containing OZ439, and 4 times for all other antimalarials. Plates were centrifuged, 190 µL of media was

carefully removed, and 190 µL of fresh media was added. Following the last wash, cultures were transferred to a new flat-bottom 96-well plate. After 72 hr, parasitemia was assessed by flow cytometry. Cultures were resuspended and 10 µL was transferred to a new 96-well plate containing 50 µL per well of 1 x PBS with 1 x SYBR Green I and 100 nM MitoTracker Deep Red. Following incubation at 37°C for 1 h, plates were read on a BD FACSCanto with a BD HTS automated plate reader and analyzed with BD FACSDiva Software version 8. Approximately 10,000 events were analyzed per well. GraphPad version 10 was used to calculate IC50 values by nonlinear regression.

For dose response assays with fixed concentrations of partner drugs, a 96-well plate was prepared containing 2-fold serial dilutions of DHA media at 100 µL per well. A bulk intermediate culture of parasites was prepared at 2% hematocrit. Partner drugs were added to this intermediate culture at 2x concentrations. After mixing, 100 µL of the intermediate culture was added to the 96-well plate containing DHA serial dilutions, for a final hematocrit of 1% and a 1 x fixed partner drug concentration.

For isobolograms, the following fixed ratios were prepared as starting concentrations: 1:0, 4:1, 2:1, 1:1, 1:2, 1:4, 0:1. The starting concentration of each drug alone (1:0 and 0:1 ratios) represents an approximate 16x IC50 concentration. Trophozoite stages were exposed to 2-fold dilutions of these ratios. Fractional IC50 (FIC50) values were calculated as follows:

$$\text{FIC50} = \frac{\text{IC50 of drugs in combination}}{\text{IC50 of individual drug}}$$

FIC50 values were plotted on an XY graph. Mean ΣFIC50 values were calculated by averaging the sums of FIC50 values from 4:1, 2:1, 1:1, 1:2, and 1:4 ratios. Trophozoite-stage IC50 values for **Figure1- figure supplement 1 and Figure 4- figure supplement 2** were obtained from 1:0 or 0:1 ratios. A one-way ANOVA with a Turkey's or Dunnett's multiple comparison test were used to assess statistical significance for IC50 values.

RSAs and Early Ring Stage Dose Response Assays. 0-3 hours post invasion (hpi) rings were obtained as previously described [124]. Briefly, schizonts were enriched using MACS LD magnet columns (Miltenyi Biotec). Schizont enriched cultures were diluted to 2% hematocrit in 3-4 mL of media and incubated for 3 h with shaking. A 5% sorbitol treatment was then used to remove remaining mature parasites. Early ring stages were seeded at 1% parasitemia and 1% hematocrit in round-bottom 96-well plates. 2-fold serial dilutions were prepared starting at 1400 nM DHA, so that both IC50 values and RSA values could be obtained. After incubation for 3 h, antimalarials

were washed out and parasitemia was assessed 72 hr later by flow cytometry as described in the previous section. GraphPad Prism version 10 was used to calculate IC50 values by nonlinear regression. RSA survival was obtained by dividing the parasitemia of cultures treated with 700 nM DHA by the untreated control. A one-way ANOVA with a Dunnett's multiple comparison test was used to determine statistical significance for IC50 values and RSA survival values.

Detection of Free Heme In Vitro. H-FluNox was kindly provided by Dr. Tasuku Hirayama (Gifu Pharmaceutical University, Lab of Pharmaceutical & Medicinal Chemistry). Reactions were carried out in a buffer containing 50 mM HEPES (pH 7.4) and 100 μM reduced glutathione. Glutathione was used to convert hemin into heme. Hemin was made up in reaction buffer and 2-fold serial dilutions were performed to obtain a range of heme concentrations starting at 500 nM. H-FluNox was used at a final concentration of 500 nM. Reactions were performed in black-walled clear-bottom 96-well plates. Following incubation with H-FluNox and indicated antimalarials at room temperature for 30 min, fluorescence was read at 485/535 nm ex/em using an EnVision Multimode Plate Reader.

Detection of Free Heme In Live Parasites. Ac-H-FluNox was kindly provided by Dr. Tasuku Hirayama (Gifu Pharmaceutical University, Lab of Pharmaceutical & Medicinal Chemistry). Parasites were synchronized to the trophozoite stage as described above. Cultures were then treated with the indicated compound for the indicated time. Media was removed and parasite cultures were resuspended and incubated in 1 x PBS containing 10 μM Ac-H-FluNox for 30 min at 37°C. Ac-H-FluNox is the cell permeable analog of H-FluNox and is converted to H-FluNox in cells [77]. Following incubation, cultures were washed with 1x PBS and then imaged using a 63× objective on a Zeiss Imager M2 Plus Widefield fluorescence microscope with AxioVision 4.8 software. Except for **Figure 3- figure supplement 1b**, a fixed exposure of 350 ms was used to capture H-FluNox fluorescence at 470/509 nm ex/em. Exposure for **Figure 3- figure supplement 1b** was adjusted for each condition so that DV staining could be optimally visualized. For quantification in **Figure 3e, 3f, 4i** and **Figure 3- figure supplement 2**, at least ten fields were captured per treatment condition and then mean fluorescence intensity of parasite minus background was quantified with ImageJ. Statistical significance of ≥ 70 parasites from at least three independent drug treatments was assessed using a one-way ANOVA.

Western Blot. Parasite drug treatment, protein harvest, sample preparation, SDS-PAGE, and wet transfer were performed as previously described [85]. Blots were blocked with 3% BSA in TBS-T and incubated overnight with primary antibodies used at 1:1000 in 1x TBS-T. Anti K48-linked ubiquitin was obtained from Cell Signaling Technologies (catalog number: D9D5, rabbit). Anti-

PMV was obtained from [125]. Blots were incubated for 1 h at room temperature with IRDye conjugated goat secondary antibodies (LICOR) at 1:10,000 dilutions. Blots were imaged using a Bio Rad imager with Image Lab Touch Software and then quantified with ImageJ. Significant differences between control and antimalarial treated parasites were determined using a one-way ANOVA with a Dunnett's multiple comparison test.

Acknowledgements

Funding for this work was provided by T32AI007172 (to D.E.G.) and F32AI188627 (to M.R.R.). We thank David Fidock (Columbia University) and Miles Siegel (LGENIA) for helpful discussion.

Contributions

This project was conceptualized by M.R.R. and D.E.G. Experimental methodology, investigation, validation, formal analysis, visualization, and writing of the original draft was done by M.R.R. Manuscript review and editing was performed by M.R.R. and D.E.G. Funding was acquired by D.E.G. and M.R.R. Supervision was provided by D.E.G.

References

1. WHO (2024). World Malaria Report.
2. Wicht, K.J., Mok, S., and Fidock, D.A. (2020). Molecular mechanisms of drug resistance in *Plasmodium falciparum* malaria. Annu Rev Microbiol *74*, 431-454. 10.1146/annurev-micro-020518-115546. PMC8130186.
3. Rosenthal, M.R. and Ng, C.L. (2020). *Plasmodium falciparum* artemisinin resistance: the effect of heme, protein damage, and parasite cell stress response. ACS Infect Dis *6*, 1599-1614. 10.1021/acsinfecdis.9b00527.
4. Sigala, P.A., Crowley, J.R., Henderson, J.P., and Goldberg, D.E. (2015). Deconvoluting heme biosynthesis to target blood-stage malaria parasites. Elife *4*. 10.7554/eLife.09143. PMC4532139.
5. Matz, J.M. (2022). *Plasmodium's* bottomless pit: properties and functions of the malaria parasite's digestive vacuole. Trends Parasitol *38*, 525-543. 10.1016/j.pt.2022.02.010.
6. Egan, T.J., Combrinck, J.M., Egan, J., Hearne, G.R., Marques, H.M., Ntenteni, S., Sewell, B.T., Smith, P.J., Taylor, D., van Schalkwyk, D.A., and Walden, J.C. (2002). Fate of haem iron in the malaria parasite *Plasmodium falciparum*. Biochem J *365*, 343-347. 10.1042/BJ20020793. PMC1222701.
7. Combrinck, J.M., Mabotha, T.E., Ncokazi, K.K., Ambele, M.A., Taylor, D., Smith, P.J., Hoppe, H.C., and Egan, T.J. (2013). Insights into the role of heme in the mechanism of action of antimalarials. ACS Chem Biol *8*, 133-137. 10.1021/cb300454t. PMC3548943.
8. Zhang, J., Krugliak, M., and Ginsburg, H. (1999). The fate of ferriprotorphyrin IX in malaria infected erythrocytes in conjunction with the mode of action of antimalarial drugs. Mol Biochem Parasitol *99*, 129-141. 10.1016/s0166-6851(99)00008-0.

9. Francis, S.E., Sullivan, D.J., Jr., and Goldberg, D.E. (1997). Hemoglobin metabolism in the malaria parasite *Plasmodium falciparum*. Annu Rev Microbiol *51*, 97-123. 10.1146/annurev.micro.51.1.97.
10. Abshire, J.R., Rowlands, C.J., Ganesan, S.M., So, P.T., and Niles, J.C. (2017). Quantification of labile heme in live malaria parasites using a genetically encoded biosensor. Proceedings of the National Academy of Sciences of the United States of America *114*, E2068-E2076. 10.1073/pnas.1615195114. PMC5358388.
11. Sullivan, D.J., Jr., Gluzman, I.Y., Russell, D.G., and Goldberg, D.E. (1996). On the molecular mechanism of chloroquine's antimalarial action. Proceedings of the National Academy of Sciences of the United States of America *93*, 11865-11870. PMC38150.
12. Sullivan, D.J., Jr., Matile, H., Ridley, R.G., and Goldberg, D.E. (1998). A common mechanism for blockade of heme polymerization by antimalarial quinolines. J Biol Chem *273*, 31103-31107. 10.1074/jbc.273.47.31103.
13. Olafson, K.N., Nguyen, T.Q., Rimer, J.D., and Vekilov, P.G. (2017). Antimalarials inhibit hematin crystallization by unique drug-surface site interactions. Proceedings of the National Academy of Sciences of the United States of America *114*, 7531-7536. 10.1073/pnas.1700125114. PMC5530657.
14. Olafson, K.N., Ketchum, M.A., Rimer, J.D., and Vekilov, P.G. (2015). Mechanisms of hematin crystallization and inhibition by the antimalarial drug chloroquine. Proceedings of the National Academy of Sciences of the United States of America *112*, 4946-4951. 10.1073/pnas.1501023112. PMC4413305.
15. Adams, P.A., Berman, P.A., Egan, T.J., Marsh, P.J., and Silver, J. (1996). The iron environment in heme and heme-antimalarial complexes of pharmacological interest. J Inorg Biochem *63*, 69-77. 10.1016/0162-0134(95)00212-x.
16. Egan, T.J., Mavuso, W.W., Ross, D.C., and Marques, H.M. (1997). Thermodynamic factors controlling the interaction of quinoline antimalarial drugs with ferriprotoporphyrin IX. J Inorg Biochem *68*, 137-145. 10.1016/s0162-0134(97)00086-x.
17. de Villiers, K.A. and Egan, T.J. (2021). Heme detoxification in the malaria parasite: A target for antimalarial drug development. Accounts of chemical research *54*, 2649-2659. 10.1021/acs.accounts.1c00154. PMC8290263.
18. Fitch, C.D. (2004). Ferriprotoporphyrin IX, phospholipids, and the antimalarial actions of quinoline drugs. Life Sci *74*, 1957-1972. 10.1016/j.lfs.2003.10.003.
19. Kapishnikov, S., Staalso, T., Yang, Y., Lee, J., Perez-Berna, A.J., Pereiro, E., Yang, Y., Werner, S., Guttmann, P., Leiserowitz, L., and Als-Nielsen, J. (2019). Mode of action of quinoline antimalarial drugs in red blood cells infected by *Plasmodium falciparum* revealed in vivo. Proceedings of the National Academy of Sciences of the United States of America *116*, 22946-22952. 10.1073/pnas.1910123116. PMC6859308.
20. Fidock, D.A., Nomura, T., Talley, A.K., Cooper, R.A., Dzekunov, S.M., Ferdig, M.T., Ursos, L.M., Sidhu, A.B., Naude, B., Deitsch, K.W., et al. (2000). Mutations in the *P. falciparum* digestive vacuole transmembrane protein PfCRT and evidence for their role in chloroquine resistance. Mol Cell *6*, 861-871. PMC2944663.
21. Kim, J., Tan, Y.Z., Wicht, K.J., Erramilli, S.K., Dhingra, S.K., Okombo, J., Vendome, J., Hagenah, L.M., Giacometti, S.I., Warren, A.L., et al. (2019). Structure and drug resistance of the *Plasmodium falciparum* transporter PfCRT. Nature *576*, 315-320. 10.1038/s41586-019-1795-x.
22. Papakrivos, J., Sa, J.M., and Wellems, T.E. (2012). Functional characterization of the *Plasmodium falciparum* chloroquine-resistance transporter (PfCRT) in transformed *Dictyostelium discoideum* vesicles. PloS one *7*, e39569. 10.1371/journal.pone.0039569. PMC3378554.

23. Sanchez, C.P., McLean, J.E., Rohrbach, P., Fidock, D.A., Stein, W.D., and Lanzer, M. (2005). Evidence for a pfcrt-associated chloroquine efflux system in the human malarial parasite *Plasmodium falciparum*. Biochemistry *44*, 9862-9870. 10.1021/bi050061f.
24. Summers, R.L., Dave, A., Dolstra, T.J., Bellanca, S., Marchetti, R.V., Nash, M.N., Richards, S.N., Goh, V., Schenk, R.L., Stein, W.D., et al. (2014). Diverse mutational pathways converge on saturable chloroquine transport via the malaria parasite's chloroquine resistance transporter. Proceedings of the National Academy of Sciences of the United States of America *111*, E1759-1767. 10.1073/pnas.1322965111. PMC4035986.
25. Cumming, J.N., Ploypradith, P., and Posner, G.H. (1997). Antimalarial activity of artemisinin (qinghaosu) and related trioxanes: mechanism(s) of action. Adv Pharmacol *37*, 253-297. 10.1016/s1054-3589(08)60952-7.
26. Meshnick, S.R., Taylor, T.E., and Kamchonwongpaisan, S. (1996). Artemisinin and the antimalarial endoperoxides: from herbal remedy to targeted chemotherapy. Microbiol Rev *60*, 301-315. 10.1128/mr.60.2.301-315.1996. PMC239445.
27. Kaiser, M., Wittlin, S., Nehrbass-Stuedli, A., Dong, Y., Wang, X., Hemphill, A., Matile, H., Brun, R., and Vennerstrom, J.L. (2007). Peroxide bond-dependent antiplasmodial specificity of artemisinin and OZ277 (RBx11160). Antimicrob Agents Chemother *51*, 2991-2993. 10.1128/AAC.00225-07. PMC1932508.
28. Zhang, S. and Gerhard, G.S. (2008). Heme activates artemisinin more efficiently than hemin, inorganic iron, or hemoglobin. Bioorg Med Chem *16*, 7853-7861. 10.1016/j.bmc.2008.02.034.
29. Meunier, B. and Robert, A. (2010). Heme as trigger and target for trioxane-containing antimalarial drugs. Accounts of chemical research *43*, 1444-1451. 10.1021/ar100070k.
30. Wang, J., Zhang, C.J., Chia, W.N., Loh, C.C., Li, Z., Lee, Y.M., He, Y., Yuan, L.X., Lim, T.K., Liu, M., et al. (2015). Haem-activated promiscuous targeting of artemisinin in *Plasmodium falciparum*. Nat Commun *6*. 10.1038/ncomms10111. 4703832.
31. Ismail, H.M., Barton, V., Phanchana, M., Charoensutthivarakul, S., Wong, M.H., Hemingway, J., Biagini, G.A., O'Neill, P.M., and Ward, S.A. (2016). Artemisinin activity-based probes identify multiple molecular targets within the asexual stage of the malaria parasites *Plasmodium falciparum* 3D7. Proceedings of the National Academy of Sciences of the United States of America *113*, 2080-2085. 10.1073/pnas.1600459113. PMC4776496.
32. Jourdan, J., Walz, A., Matile, H., Schmidt, A., Wu, J., Wang, X., Dong, Y., Vennerstrom, J.L., Schmidt, R.S., Wittlin, S., and Maser, P. (2019). Stochastic protein alkylation by antimalarial peroxides. ACS Infect Dis *5*, 2067-2075. 10.1021/acsinfecdis.9b00264.
33. Ariey, F., Witkowski, B., Amaratunga, C., Beghain, J., Langlois, A.C., Khim, N., Kim, S., Duru, V., Bouchier, C., Ma, L., et al. (2014). A molecular marker of artemisinin-resistant *Plasmodium falciparum* malaria. Nature *505*, 50-55. 10.1038/nature12876. 24352242.
34. Ashley, E.A., Dhorda, M., Fairhurst, R.M., Amaratunga, C., Lim, P., Suon, S., Sreng, S., Anderson, J.M., Mao, S., Sam, B., et al. (2014). Spread of artemisinin resistance in *Plasmodium falciparum* malaria. N Engl J Med *371*, 411-423. 10.1056/NEJMoa1314981. 4143591.
35. Straimer, J., Gnadig, N.F., Witkowski, B., Amaratunga, C., Duru, V., Ramadani, A.P., Dacheux, M., Khim, N., Zhang, L., Lam, S., et al. (2015). K13-propeller mutations confer artemisinin resistance in *Plasmodium falciparum* clinical isolates. Science *347*, 428-431. 10.1126/science.1260867. 4349400.
36. Birnbaum, J., Scharf, S., Schmidt, S., Jonscher, E., Hoeijmakers, W.A.M., Flemming, S., Toenhake, C.G., Schmitt, M., Sabitzki, R., Bergmann, B., et al. (2020). A Kelch13-defined endocytosis pathway mediates artemisinin resistance in malaria parasites. Science *367*, 51-59. 10.1126/science.aax4735.

37. Siddiqui, G., Srivastava, A., Russell, A.S., and Creek, D.J. (2017). Multi-omics based identification of specific biochemical changes associated with PfKelch13-mutant artemisinin-resistant *Plasmodium falciparum*. J Infect Dis *215*, 1435-1444. 10.1093/infdis/jix156.
38. Yang, T., Yeoh, L.M., Tutor, M.V., Dixon, M.W., McMillan, P.J., Xie, S.C., Bridgford, J.L., Gillett, D.L., Duffy, M.F., Ralph, S.A., et al. (2019). Decreased K13 abundance reduces hemoglobin catabolism and proteotoxic stress, underpinning artemisinin resistance. Cell Rep *29*, 2917-2928 e2915. 10.1016/j.celrep.2019.10.095.
39. Uwimana, A., Legrand, E., Stokes, B.H., Ndikumana, J.M., Warsame, M., Umulisa, N., Ngamije, D., Munyaneza, T., Mazarati, J.B., Munguti, K., et al. (2020). Emergence and clonal expansion of in vitro artemisinin-resistant *Plasmodium falciparum* kelch13 R561H mutant parasites in Rwanda. Nat Med *26*, 1602-1608. 10.1038/s41591-020-1005-2.
40. Uwimana, A., Umulisa, N., Venkatesan, M., Svigel, S.S., Zhou, Z., Munyaneza, T., Habimana, R.M., Rucogoza, A., Moriarty, L.F., Sandford, R., et al. (2021). Association of *Plasmodium falciparum* kelch13 R561H genotypes with delayed parasite clearance in Rwanda: an open-label, single-arm, multicentre, therapeutic efficacy study. Lancet Infect Dis *21*, 1120-1128. 10.1016/S1473-3099(21)00142-0.
41. Tumwebaze, P.K., Conrad, M.D., Okitwi, M., Orena, S., Byaruhanga, O., Katairo, T., Legac, J., Garg, S., Giesbrecht, D., Smith, S.R., et al. (2022). Decreased susceptibility of *Plasmodium falciparum* to both dihydroartemisinin and lumefantrine in northern Uganda. Nat Commun *13*, 6353. 10.1038/s41467-022-33873-x. PMC9605985.
42. Rosenthal, P.J., Asua, V., Bailey, J.A., Conrad, M.D., Ishengoma, D.S., Kamya, M.R., Rasmussen, C., Tadesse, F.G., Uwimana, A., and Fidock, D.A. (2024). The emergence of artemisinin partial resistance in Africa: how do we respond? Lancet Infect Dis *24*, e591-e600. 10.1016/S1473-3099(24)00141-5.
43. Saunders, D.L., Vanachayangkul, P., Lon, C., Program, U.S.A.M.M.R., National Center for Parasitology, E., Malaria, C., and Royal Cambodian Armed, F. (2014). Dihydroartemisinin-piperaquine failure in Cambodia. N Engl J Med *371*, 484-485. 10.1056/NEJMc1403007.
44. Spring, M.D., Lin, J.T., Manning, J.E., Vanachayangkul, P., Somethy, S., Bun, R., Se, Y., Chann, S., Ittiverakul, M., Sia-ngam, P., et al. (2015). Dihydroartemisinin-piperaquine failure associated with a triple mutant including kelch13 C580Y in Cambodia: an observational cohort study. Lancet Infect Dis *15*, 683-691. 10.1016/S1473-3099(15)70049-6.
45. Leang, R., Taylor, W.R., Bouth, D.M., Song, L., Tarning, J., Char, M.C., Kim, S., Witkowski, B., Duru, V., Domergue, A., et al. (2015). Evidence of *Plasmodium falciparum* malaria multidrug resistance to artemisinin and piperaquine in Western Cambodia: dihydroartemisinin-piperaquine open-label multicenter clinical assessment. Antimicrob Agents Chemother *59*, 4719-4726. 10.1128/AAC.00835-15. PMC4505193.
46. van der Pluijm, R.W., Imwong, M., Chau, N.H., Hoa, N.T., Thuy-Nhien, N.T., Thanh, N.V., Jittamala, P., Hanboonkunupakarn, B., Chutasmit, K., Saelow, C., et al. (2019). Determinants of dihydroartemisinin-piperaquine treatment failure in *Plasmodium falciparum* malaria in Cambodia, Thailand, and Vietnam: a prospective clinical, pharmacological, and genetic study. Lancet Infect Dis *19*, 952-961. 10.1016/S1473-3099(19)30391-3. PMC6715822.
47. van der Pluijm, R.W., Tripura, R., Hoglund, R.M., Pyae Phyo, A., Lek, D., Ul Islam, A., Anvikar, A.R., Satpathi, P., Satpathi, S., Behera, P.K., et al. (2020). Triple artemisinin-based combination therapies versus artemisinin-based combination therapies for uncomplicated Plasmodium falciparum malaria: a multicentre, open-label, randomised clinical trial. Lancet *395*, 1345-1360. 10.1016/S0140-6736(20)30552-3. PMC8204272.

48. Liu, H., Xu, J.W., Deng, D.W., Wang, H.Y., Nie, R.H., Yin, Y.J., and Li, M. (2023). Dihydroartemisinin-piperaquine efficacy in *Plasmodium falciparum* treatment and prevalence of drug-resistant molecular markers along China-Myanmar border in 2014-2023. J Glob Antimicrob Resist *35*, 271-278. 10.1016/j.jgar.2023.10.001.
49. Amaratunga, C., Lim, P., Suon, S., Sreng, S., Mao, S., Sopha, C., Sam, B., Dek, D., Try, V., Amato, R., et al. (2016). Dihydroartemisinin-piperaquine resistance in *Plasmodium falciparum* malaria in Cambodia: a multisite prospective cohort study. Lancet Infect Dis *16*, 357-365. 10.1016/S1473-3099(15)00487-9. PMC4792715.
50. Phyo, A.P., Ashley, E.A., Anderson, T.J.C., Bozdech, Z., Carrara, V.I., Sriprawat, K., Nair, S., White, M.M., Dziekan, J., Ling, C., et al. (2016). Declining efficacy of artemisinin combination therapy against *P. falciparum* malaria on the Thai-Myanmar border (2003-2013): the role of parasite genetic factors. Clin Infect Dis *63*, 784-791. 10.1093/cid/ciw388. PMC4996140.
51. Mairet-Khedim, M., Leang, R., Marmai, C., Khim, N., Kim, S., Ke, S., Kauy, C., Kloeung, N., Eam, R., Chy, S., et al. (2021). Clinical and in vitro resistance of *Plasmodium falciparum* to artesunate-amodiaquine in Cambodia. Clin Infect Dis *73*, 406-413. 10.1093/cid/ciaa628. PMC8326543.
52. Davis, T.M., Hamzah, J., Ilett, K.F., Karunajeewa, H.A., Reeder, J.C., Batty, K.T., Hackett, S., and Barrett, P.H. (2006). In vitro interactions between piperaquine, dihydroartemisinin, and other conventional and novel antimalarial drugs. Antimicrob Agents Chemother *50*, 2883-2885. 10.1128/AAC.00177-06. PMC1538683.
53. Fivelman, Q.L., Walden, J.C., Smith, P.J., Folb, P.I., and Barnes, K.I. (1999). The effect of artesunate combined with standard antimalarials against chloroquine-sensitive and chloroquine-resistant strains of *Plasmodium falciparum* in vitro. Trans R Soc Trop Med Hyg *93*, 429-432. 10.1016/s0035-9203(99)90147-5.
54. Ribbiso, K.A., Heller, L.E., Taye, A., Julian, E., Willems, A.V., and Roepe, P.D. (2021). Artemisinin-based drugs target the *Plasmodium falciparum* heme detoxification pathway. Antimicrob Agents Chemother *65*. 10.1128/AAC.02137-20. PMC8097475.
55. Ansbro, M.R., Itkin, Z., Chen, L., Zahoranszky-Kohalmi, G., Amaratunga, C., Miotto, O., Peryea, T., Hobbs, C.V., Suon, S., Sa, J.M., et al. (2020). Modulation of triple artemisinin-based combination therapy pharmacodynamics by *Plasmodium falciparum* genotype. ACS Pharmacol Transl Sci *3*, 1144-1157. 10.1021/acsptsci.0c00110. PMC7737215.
56. Muangnoicharoen, S., Johnson, D.J., Looareesuwan, S., Krudsood, S., and Ward, S.A. (2009). Role of known molecular markers of resistance in the antimalarial potency of piperaquine and dihydroartemisinin in vitro. Antimicrob Agents Chemother *53*, 1362-1366. 10.1128/AAC.01656-08. PMC2663099.
57. Duru, V., Khim, N., Leang, R., Kim, S., Domergue, A., Kloeung, N., Ke, S., Chy, S., Eam, R., Khean, C., et al. (2015). *Plasmodium falciparum* dihydroartemisinin-piperaquine failures in Cambodia are associated with mutant K13 parasites presenting high survival rates in novel piperaquine *in vitro* assays: retrospective and prospective investigations. BMC Med *13*, 305. 10.1186/s12916-015-0539-5. 4688949.
58. Witkowski, B., Amaratunga, C., Khim, N., Sreng, S., Chim, P., Kim, S., Lim, P., Mao, S., Sopha, C., Sam, B., et al. (2013). Novel phenotypic assays for the detection of artemisinin-resistant *Plasmodium falciparum* malaria in Cambodia: in-vitro and ex-vivo drug-response studies. Lancet Infect Dis *13*, 1043-1049. 10.1016/S1473-3099(13)70252-4. PMC5015432.
59. Stokes, B.H., Yoo, E., Murithi, J.M., Luth, M.R., Afanasyev, P., da Fonseca, P.C.A., Winzeler, E.A., Ng, C.L., Bogyo, M., and Fidock, D.A. (2019). Covalent *Plasmodium falciparum*-selective proteasome inhibitors exhibit a low propensity for generating

resistance *in vitro* and synergize with multiple antimalarial agents. PLoS Pathog *15*, e1007722-e1107750. 10.1371/journal.ppat.1007722. PMC6553790.
60. Gligorijevic, B., Purdy, K., Elliott, D.A., Cooper, R.A., and Roepe, P.D. (2008). Stage independent chloroquine resistance and chloroquine toxicity revealed via spinning disk confocal microscopy. Mol Biochem Parasitol *159*, 7-23. 10.1016/j.molbiopara.2007.12.014. PMC2440633.
61. Rosenthal, M.R. and Ng, C.L. (2021). A proteasome mutation sensitizes *P. falciparum* Cam3.II K13(C580Y) parasites to DHA and OZ439. ACS Infect Dis. 10.1021/acsinfecdis.0c00900.
62. Eastman, R.T., Khine, P., Huang, R., Thomas, C.J., and Su, X.Z. (2016). PfCRT and PfMDR1 modulate interactions of artemisinin derivatives and ion channel blockers. Sci Rep *6*, 25379. 10.1038/srep25379. PMC4857081.
63. Straimer, J., Lee, M.C., Lee, A.H., Zeitler, B., Williams, A.E., Pearl, J.R., Zhang, L., Rebar, E.J., Gregory, P.D., Llinas, M., et al. (2012). Site-specific genome editing in *Plasmodium falciparum* using engineered zinc-finger nucleases. Nat Methods *9*, 993-998. 10.1038/nmeth.2143. 3697006.
64. Ross, L.S., Dhingra, S.K., Mok, S., Yeo, T., Wicht, K.J., Kumpornsin, K., Takala-Harrison, S., Witkowski, B., Fairhurst, R.M., Ariey, F., et al. (2018). Emerging Southeast Asian PfCRT mutations confer *Plasmodium falciparum* resistance to the first-line antimalarial piperaquine. Nat Commun *9*, 3314. 10.1038/s41467-018-05652-0. PMC6095916.
65. Vanaerschot, M., Lucantoni, L., Li, T., Combrinck, J.M., Ruecker, A., Kumar, T.R.S., Rubiano, K., Ferreira, P.E., Siciliano, G., Gulati, S., et al. (2017). Hexahydroquinolines are antimalarial candidates with potent blood-stage and transmission-blocking activity. Nat Microbiol *2*, 1403-1414. 10.1038/s41564-017-0007-4. PMC5708124.
66. Wang, Z., Cabrera, M., Yang, J., Yuan, L., Gupta, B., Liang, X., Kemirembe, K., Shrestha, S., Brashear, A., Li, X., et al. (2016). Genome-wide association analysis identifies genetic loci associated with resistance to multiple antimalarials in *Plasmodium falciparum* from China-Myanmar border. Sci Rep *6*. 10.1038/srep33891. PMC5046179.
67. Cabrera, M., Paguio, M.F., Xie, C., and Roepe, P.D. (2009). Reduced digestive vacuolar accumulation of chloroquine is not linked to resistance to chloroquine toxicity. Biochemistry *48*, 11152-11154. 10.1021/bi901765v. PMC2788207.
68. Melo, M.M., Costa, M.R.F., Filho, F.S.S., Brito-Sousa, J.D., Almeida, A.C.G., Monteiro, W.M., Melo, G.C., Vieira, J.L.F., and Alecrim, M. (2022). Pharmacokinetics of chloroquine in patients with malaria by *P. vivax* from the Western Brazilian Amazon basin. Biomed Pharmacother *149*, 112874. 10.1016/j.biopha.2022.112874.
69. Nguyen, D.V., Nguyen, Q.P., Nguyen, N.D., Le, T.T., Nguyen, T.D., Dinh, D.N., Nguyen, T.X., Bui, D., Chavchich, M., and Edstein, M.D. (2009). Pharmacokinetics and ex vivo pharmacodynamic antimalarial activity of dihydroartemisinin-piperaquine in patients with uncomplicated falciparum malaria in Vietnam. Antimicrob Agents Chemother *53*, 3534-3537. 10.1128/AAC.01717-08. PMC2715592.
70. Hoglund, R.M., Workman, L., Edstein, M.D., Thanh, N.X., Quang, N.N., Zongo, I., Ouedraogo, J.B., Borrmann, S., Mwai, L., Nsanzabana, C., et al. (2017). Population pharmacokinetic properties of piperaquine in falciparum malaria: An individual participant data meta-analysis. PLoS Med *14*, e1002212. 10.1371/journal.pmed.1002212. PMC5224788.
71. Nkhoma, S.C., Ahmed, A.O.A., Zaman, S., Porier, D., Baker, Z., and Stedman, T.T. (2021). Dissection of haplotype-specific drug response phenotypes in multiclonal malaria isolates. International journal for parasitology. Drugs and drug resistance *15*, 152-161. 10.1016/j.ijpddr.2021.03.001. PMC8039770.

72. Kuter, D., Streltsov, V., Davydova, N., Venter, G.A., Naidoo, K.J., and Egan, T.J. (2016). Solution structures of chloroquine-ferriheme complexes modeled using MD simulation and investigated by EXAFS spectroscopy. J Inorg Biochem *154*, 114-125. 10.1016/j.jinorgbio.2015.06.010.
73. Dorn, A., Vippagunta, S.R., Matile, H., Jaquet, C., Vennerstrom, J.L., and Ridley, R.G. (1998). An assessment of drug-haematin binding as a mechanism for inhibition of haematin polymerisation by quinoline antimalarials. Biochemical pharmacology *55*, 727-736. 10.1016/s0006-2952(97)00510-8.
74. Leed, A., DuBay, K., Ursos, L.M., Sears, D., De Dios, A.C., and Roepe, P.D. (2002). Solution structures of antimalarial drug-heme complexes. Biochemistry *41*, 10245-10255. 10.1021/bi020195i.
75. Egan, T.J. (2006). Interactions of quinoline antimalarials with hematin in solution. J Inorg Biochem *100*, 916-926. 10.1016/j.jinorgbio.2005.11.005.
76. Vippagunta, S.R., Dorn, A., Ridley, R.G., and Vennerstrom, J.L. (2000). Characterization of chloroquine-hematin mu-oxo dimer binding by isothermal titration calorimetry. Biochim Biophys Acta *1475*, 133-140. 10.1016/s0304-4165(00)00058-1.
77. Kawai, K., Hirayama, T., Imai, H., Murakami, T., Inden, M., Hozumi, I., and Nagasawa, H. (2022). Molecular imaging of labile heme in living cells using a small molecule fluorescent probe. J Am Chem Soc *144*, 3793-3803. 10.1021/jacs.1c08485.
78. Gutman, J., Green, M., Durand, S., Rojas, O.V., Ganguly, B., Quezada, W.M., Utz, G.C., Slutsker, L., Ruebush, T.K., 2nd, and Bacon, D.J. (2009). Mefloquine pharmacokinetics and mefloquine-artesunate effectiveness in Peruvian patients with uncomplicated *Plasmodium falciparum* malaria. Malar J *8*, 58. 10.1186/1475-2875-8-58. PMC2674465.
79. Wiser, M.F. (2024). The digestive vacuole of the malaria parasite: A specialized lysosome. Pathogens *13*. 10.3390/pathogens13030182. PMC10974218.
80. Yayon, A., Cabantchik, Z.I., and Ginsburg, H. (1984). Identification of the acidic compartment of *Plasmodium falciparum*-infected human erythrocytes as the target of the antimalarial drug chloroquine. The EMBO journal *3*, 2695-2700. 10.1002/j.1460-2075.1984.tb02195.x. PMC557751.
81. Dhingra, S.K., Redhi, D., Combrinck, J.M., Yeo, T., Okombo, J., Henrich, P.P., Cowell, A.N., Gupta, P., Stegman, M.L., Hoke, J.M., et al. (2017). A variant PfCRT isoform can contribute to *Plasmodium falciparum* resistance to the first-line partner drug piperaquine. mBio *8*. 10.1128/mBio.00303-17. PMC5424201.
82. Warhurst, D.C., Craig, J.C., Adagu, I.S., Guy, R.K., Madrid, P.B., and Fivelman, Q.L. (2007). Activity of piperaquine and other 4-aminoquinoline antiplasmodial drugs against chloroquine-sensitive and resistant blood-stages of *Plasmodium falciparum*. Role of beta-haematin inhibition and drug concentration in vacuolar water- and lipid-phases. Biochemical pharmacology *73*, 1910-1926. 10.1016/j.bcp.2007.03.011.
83. Combrinck, J.M., Fong, K.Y., Gibhard, L., Smith, P.J., Wright, D.W., and Egan, T.J. (2015). Optimization of a multi-well colorimetric assay to determine haem species in *Plasmodium falciparum* in the presence of anti-malarials. Malar J *14*, 253. 10.1186/s12936-015-0729-9. PMC4484700.
84. Bridgford, J.L., Xie, S.C., Cobbold, S.A., Pasaje, C.F.A., Herrmann, S., Yang, T., Gillett, D.L., Dick, L.R., Ralph, S.A., Dogovski, C., et al. (2018). Artemisinin kills malaria parasites by damaging proteins and inhibiting the proteasome. Nat Commun *9*, 3801. 10.1038/s41467-018-06221-1. PMC6143634.
85. Rosenthal, M.R., Vijayrajratnam, S., Firestone, T.M., and Ng, C.L. (2024). Enhanced cell stress response and protein degradation capacity underlie artemisinin resistance in *Plasmodium falciparum*. mSphere *9*, e0037124. 10.1128/msphere.00371-24. PMC11580438.

86. Coulibaly, B., Pritsch, M., Bountogo, M., Meissner, P.E., Nebie, E., Klose, C., Kieser, M., Berens-Riha, N., Wieser, A., Sirima, S.B., et al. (2015). Efficacy and safety of triple combination therapy with artesunate-amodiaquine-methylene blue for falciparum malaria in children: a randomized controlled trial in Burkina Faso. J Infect Dis *211*, 689-697. 10.1093/infdis/jiu540.
87. Peto, T.J., Tripura, R., Callery, J.J., Lek, D., Nghia, H.D.T., Nguon, C., Thuong, N.T.H., van der Pluijm, R.W., Dung, N.T.P., Sokha, M., et al. (2022). Triple therapy with artemether-lumefantrine plus amodiaquine versus artemether-lumefantrine alone for artemisinin-resistant, uncomplicated *falciparum* malaria: an open-label, randomised, multicentre trial. Lancet Infect Dis *22*, 867-878. 10.1016/S1473-3099(21)00692-7. PMC9132777.
88. Mahamar, A., Vanheer, L.N., Smit, M.J., Sanogo, K., Sinaba, Y., Niambele, S.M., Diallo, M., Dicko, O.M., Diarra, R.S., Maguiraga, S.O., et al. (2024). Artemether-lumefantrine-amodiaquine or artesunate-amodiaquine combined with single low-dose primaquine to reduce *Plasmodium falciparum* malaria transmission in Ouelessebougou, Mali: a five-arm, phase 2, single-blind, randomised controlled trial. Lancet Microbe, 100966. 10.1016/j.lanmic.2024.100966.
89. Phyo, A.P., Jittamala, P., Nosten, F.H., Pukrittayakamee, S., Imwong, M., White, N.J., Duparc, S., Macintyre, F., Baker, M., and Mohrle, J.J. (2016). Antimalarial activity of artefenomel (OZ439), a novel synthetic antimalarial endoperoxide, in patients with *Plasmodium falciparum* and *Plasmodium vivax* malaria: an open-label phase 2 trial. Lancet Infect Dis *16*, 61-69. 10.1016/S1473-3099(15)00320-5. PMC4700386.
90. Macintyre, F., Adoke, Y., Tiono, A.B., Duong, T.T., Mombo-Ngoma, G., Bouyou-Akotet, M., Tinto, H., Bassat, Q., Issifou, S., Adamy, M., et al. (2017). A randomised, double-blind clinical phase II trial of the efficacy, safety, tolerability and pharmacokinetics of a single dose combination treatment with artefenomel and piperaquine in adults and children with uncomplicated *Plasmodium falciparum* malaria. BMC Med *15*, 181. 10.1186/s12916-017-0940-3. PMC5632828.
91. Adoke, Y., Zoleko-Manego, R., Ouoba, S., Tiono, A.B., Kaguthi, G., Bonzela, J.E., Duong, T.T., Nahum, A., Bouyou-Akotet, M., Ogutu, B., et al. (2021). A randomized, double-blind, phase 2b study to investigate the efficacy, safety, tolerability and pharmacokinetics of a single-dose regimen of ferroquine with artefenomel in adults and children with uncomplicated *Plasmodium falciparum* malaria. Malar J *20*, 222. 10.1186/s12936-021-03749-4. PMC8135182.
92. Gansane, A., Lingani, M., Yeka, A., Nahum, A., Bouyou-Akotet, M., Mombo-Ngoma, G., Kaguthi, G., Barcelo, C., Laurijssens, B., Cantalloube, C., et al. (2023). Randomized, open-label, phase 2a study to evaluate the contribution of artefenomel to the clinical and parasiticidal activity of artefenomel plus ferroquine in African patients with uncomplicated *Plasmodium falciparum* malaria. Malar J *22*, 2. 10.1186/s12936-022-04420-2. PMC9809015.
93. Hamilton, W.L., Amato, R., van der Pluijm, R.W., Jacob, C.G., Quang, H.H., Thuy-Nhien, N.T., Hien, T.T., Hongvanthong, B., Chindavongsa, K., Mayxay, M., et al. (2019). Evolution and expansion of multidrug-resistant malaria in southeast Asia: a genomic epidemiology study. Lancet Infect Dis *19*, 943-951. 10.1016/S1473-3099(19)30392-5. PMC6715858.
94. Phuc, B.Q., Rasmussen, C., Duong, T.T., Dong, L.T., Loi, M.A., Menard, D., Tarning, J., Bustos, D., Ringwald, P., Galappaththy, G.L., and Thieu, N.Q. (2017). Treatment failure of dihydroartemisinin/piperaquine for *Plasmodium falciparum* malaria, Vietnam. Emerging infectious diseases *23*, 715-717. 10.3201/eid2304.161872. 5367417.
95. Biot, C., Taramelli, D., Forfar-Bares, I., Maciejewski, L.A., Boyce, M., Nowogrocki, G., Brocard, J.S., Basilico, N., Olliaro, P., and Egan, T.J. (2005). Insights into the

mechanism of action of ferroquine. Relationship between physicochemical properties and antiplasmodial activity. Mol Pharm *2*, 185-193. 10.1021/mp0500061.
96. Wang, J., Huang, L., Li, J., Fan, Q., Long, Y., Li, Y., and Zhou, B. (2010). Artemisinin directly targets malarial mitochondria through its specific mitochondrial activation. PloS one *5*, e9582. 10.1371/journal.pone.0009582. PMC2833198.
97. Gao, P., Wang, J., Qiu, C., Zhang, H., Wang, C., Zhang, Y., Sun, P., Chen, H., Wong, Y.K., Chen, J., et al. (2024). Photoaffinity probe-based antimalarial target identification of artemisinin in the intraerythrocytic developmental cycle of *Plasmodium falciparum*. Imeta *3*, e176. 10.1002/imt2.176. PMC11170969.
98. Ismail, H.M., Barton, V.E., Panchana, M., Charoensutthivarakul, S., Biagini, G.A., Ward, S.A., and O'Neill, P.M. (2016). A click chemistry-based proteomic approach reveals that 1,2,4-trioxolane and artemisinin antimalarials share a common protein alkylation profile. Angewandte Chemie *55*, 6401-6405. 10.1002/anie.201512062. 4934138.
99. Siddiqui, G., Giannangelo, C., De Paoli, A., Schuh, A.K., Heimsch, K.C., Anderson, D., Brown, T.G., MacRaild, C.A., Wu, J., Wang, X., et al. (2022). Peroxide antimalarial drugs target redox homeostasis in *Plasmodium falciparum* infected red blood cells. ACS Infect Dis *8*, 210-226. 10.1021/acsinfecdis.1c00550. PMC8762662.
100. Jourdan, J., Matile, H., Reift, E., Biehlmaier, O., Dong, Y., Wang, X., Maser, P., Vennerstrom, J.L., and Wittlin, S. (2016). Monoclonal antibodies that recognize the alkylation signature of antimalarial ozonides OZ277 (arterolane) and OZ439 (artefenomel). ACS Infect Dis *2*, 54-61. 10.1021/acsinfecdis.5b00090. 4718528.
101. Famin, O. and Ginsburg, H. (2003). The treatment of *Plasmodium falciparum*-infected erythrocytes with chloroquine leads to accumulation of ferriprotoporphyrin IX bound to particular parasite proteins and to the inhibition of the parasite's 6-phosphogluconate dehydrogenase. Parasite *10*, 39-50. 10.1051/parasite/2003101p39.
102. Sidhu, A.B., Uhlemann, A.C., Valderramos, S.G., Valderramos, J.C., Krishna, S., and Fidock, D.A. (2006). Decreasing *pfmdr1* copy number in *Plasmodium falciparum* malaria heightens susceptibility to mefloquine, lumefantrine, halofantrine, quinine, and artemisinin. J Infect Dis *194*, 528-535. 10.1086/507115. PMC2978021.
103. Rohrbach, P., Sanchez, C.P., Hayton, K., Friedrich, O., Patel, J., Sidhu, A.B., Ferdig, M.T., Fidock, D.A., and Lanzer, M. (2006). Genetic linkage of pfmdr1 with food vacuolar solute import in *Plasmodium falciparum*. The EMBO journal *25*, 3000-3011. 10.1038/sj.emboj.7601203. PMC1500988.
104. Wong, W., Bai, X.C., Sleebs, B.E., Triglia, T., Brown, A., Thompson, J.K., Jackson, K.E., Hanssen, E., Marapana, D.S., Fernandez, I.S., et al. (2017). Mefloquine targets the *Plasmodium falciparum* 80S ribosome to inhibit protein synthesis. Nat Microbiol *2*, 17031. 10.1038/nmicrobiol.2017.31. PMC5439513.
105. Packard, R.M. (2014). The origins of antimalarial-drug resistance. N Engl J Med *371*, 397-399. 10.1056/NEJMp1403340.
106. Sutherland, C.J., Drakeley, C.J., Obisike, U., Coleman, R., Jawara, M., Targett, G.A., Milligan, P., Pinder, M., and Walraven, G. (2003). The addition of artesunate to chloroquine for treatment of *Plasmodium falciparum* malaria in Gambian children delays, but does not prevent treatment failure. Am J Trop Med Hyg *69*, 19-25.
107. Kofoed, P.E., Poulsen, A., Co, F., Hedegaard, K., Aaby, P., and Rombo, L. (2003). No benefits from combining chloroquine with artesunate for three days for treatment of *Plasmodium falciparum* in Guinea-Bissau. Trans R Soc Trop Med Hyg *97*, 429-433. 10.1016/s0035-9203(03)90078-2.
108. Sirima, S.B., Tiono, A.B., Konate, A., Diarra, A., Castelli, F., Pinoges, L., Mugittu, K., Taylor, W.R., and Olliaros, P.L. (2003). Efficacy of artesunate plus chloroquine for the treatment of uncomplicated malaria in children in Burkina Faso: a double-blind,

randomized, controlled trial. Trans R Soc Trop Med Hyg *97*, 345-349. 10.1016/s0035-9203(03)90166-0.
109. von Seidlein, L., Jawara, M., Coleman, R., Doherty, T., Walraven, G., and Targett, G. (2001). Parasitaemia and gametocytaemia after treatment with chloroquine, pyrimethamine/sulfadoxine, and pyrimethamine/sulfadoxine combined with artesunate in young Gambians with uncomplicated malaria. Trop Med Int Health *6*, 92-98. 10.1046/j.1365-3156.2001.00683.x.
110. Mutabingwa, T.K., Anthony, D., Heller, A., Hallett, R., Ahmed, J., Drakeley, C., Greenwood, B.M., and Whitty, C.J. (2005). Amodiaquine alone, amodiaquine+sulfadoxine-pyrimethamine, amodiaquine+artesunate, and artemether-lumefantrine for outpatient treatment of malaria in Tanzanian children: a four-arm randomised effectiveness trial. Lancet *365*, 1474-1480. 10.1016/S0140-6736(05)66417-3.
111. Nguyen, T.D., Gao, B., Amaratunga, C., Dhorda, M., Tran, T.N., White, N.J., Dondorp, A.M., Boni, M.F., and Aguas, R. (2023). Preventing antimalarial drug resistance with triple artemisinin-based combination therapies. Nat Commun *14*, 4568. 10.1038/s41467-023-39914-3. PMC10387089.
112. van der Pluijm, R.W., Amaratunga, C., Dhorda, M., and Dondorp, A.M. (2021). Triple artemisinin-based combination therapies for malaria - A new paradigm? Trends Parasitol *37*, 15-24. 10.1016/j.pt.2020.09.011.
113. Wang, J., Xu, C., Wong, Y.K., Ma, N., Liao, F.L., Jiang, T., and Tu, Y. (2021). Triple artemisinin-based combination therapies for malaria: proceed with caution. Lancet *396*, 1976. 10.1016/S0140-6736(20)32400-4.
114. Amato, R., Lim, P., Miotto, O., Amaratunga, C., Dek, D., Pearson, R.D., Almagro-Garcia, J., Neal, A.T., Sreng, S., Suon, S., et al. (2017). Genetic markers associated with dihydroartemisinin-piperaquine failure in *Plasmodium falciparum* malaria in Cambodia: a genotype-phenotype association study. Lancet Infect Dis *17*, 164-173. 10.1016/S1473-3099(16)30409-1.
115. Witkowski, B., Duru, V., Khim, N., Ross, L.S., Saintpierre, B., Beghain, J., Chy, S., Kim, S., Ke, S., Kloeung, N., et al. (2017). A surrogate marker of piperaquine-resistant *Plasmodium falciparum* malaria: a phenotype-genotype association study. Lancet Infect Dis *17*, 174-183. 10.1016/S1473-3099(16)30415-7. PMC5266792.
116. Rossi, G., De Smet, M., Khim, N., Kindermans, J.M., and Menard, D. (2017). Emergence of *Plasmodium falciparum* triple mutant in Cambodia. Lancet Infect Dis *17*, 1233. 10.1016/S1473-3099(17)30635-7.
117. Palmer, K.J., Holliday, S.M., and Brogden, R.N. (1993). Mefloquine. A review of its antimalarial activity, pharmacokinetic properties and therapeutic efficacy. Drugs *45*, 430-475. 10.2165/00003495-199345030-00009.
118. Rijken, M.J., McGready, R., Phyo, A.P., Lindegardh, N., Tarning, J., Laochan, N., Than, H.H., Mu, O., Win, A.K., Singhasivanon, P., et al. (2011). Pharmacokinetics of dihydroartemisinin and piperaquine in pregnant and nonpregnant women with uncomplicated falciparum malaria. Antimicrob Agents Chemother *55*, 5500-5506. 10.1128/AAC.05067-11. PMC3232755.
119. Walz, A., Leroy, D., Andenmatten, N., Maser, P., and Wittlin, S. (2019). Anti-malarial ozonides OZ439 and OZ609 tested at clinically relevant compound exposure parameters in a novel ring-stage survival assay. Malar J *18*, 427. 10.1186/s12936-019-3056-8. PMC6918666.
120. Baumgartner, F., Jourdan, J., Scheurer, C., Blasco, B., Campo, B., Maser, P., and Wittlin, S. (2017). In vitro activity of anti-malarial ozonides against an artemisinin-resistant isolate. Malar J *16*, 45. 10.1186/s12936-017-1696-0. PMC5267415.

121. Straimer, J., Gnadig, N.F., Stokes, B.H., Ehrenberger, M., Crane, A.A., and Fidock, D.A. (2017). *Plasmodium falciparum* K13 mutations differentially impact ozonide susceptibility and parasite fitness *in vitro*. MBio *8*. 10.1128/mBio.00172-17. PMC5388803.
122. Supan, C., Mombo-Ngoma, G., Kombila, M., Ospina Salazar, C.L., Held, J., Lell, B., Cantalloube, C., Djeriou, E., Ogutu, B., Waitumbi, J., et al. (2017). Phase 2a, open-label, 4-escalating-dose, randomized multicenter study evaluating the safety and activity of ferroquine (SSR97193) plus artesunate, versus amodiaquine plus artesunate, in African adult men with uncomplicated *Plasmodium falciparum* malaria. Am J Trop Med Hyg *97*, 514-525. 10.4269/ajtmh.16-0731. PMC5544076.
123. Demarta-Gatsi, C., Andenmatten, N., Jimenez-Diaz, M.B., Gobeau, N., Cherkaoui-Rabti, M.H., Fuchs, A., Diaz, P., Berja, S., Sanchez, R., Gomez, H., et al. (2023). Predicting optimal antimalarial drug combinations from a standardized *Plasmodium falciparum* humanized mouse model. Antimicrob Agents Chemother *67*, e0157422. 10.1128/aac.01574-22. PMC10269072.
124. Hasan, M.M., Polino, A.J., Mukherjee, S., Vaupel, B., and Goldberg, D.E. (2023). The mature N-termini of *Plasmodium* effector proteins confer specificity of export. mBio *14*, e0121523. 10.1128/mbio.01215-23. PMC10653839.
125. Banerjee, R., Liu, J., Beatty, W., Pelosof, L., Klemba, M., and Goldberg, D.E. (2002). Four plasmepsins are active in the *Plasmodium falciparum* food vacuole, including a protease with an active-site histidine. Proceedings of the National Academy of Sciences of the United States of America *99*, 990-995. 10.1073/pnas.022630099. PMC117418.

Figure 1

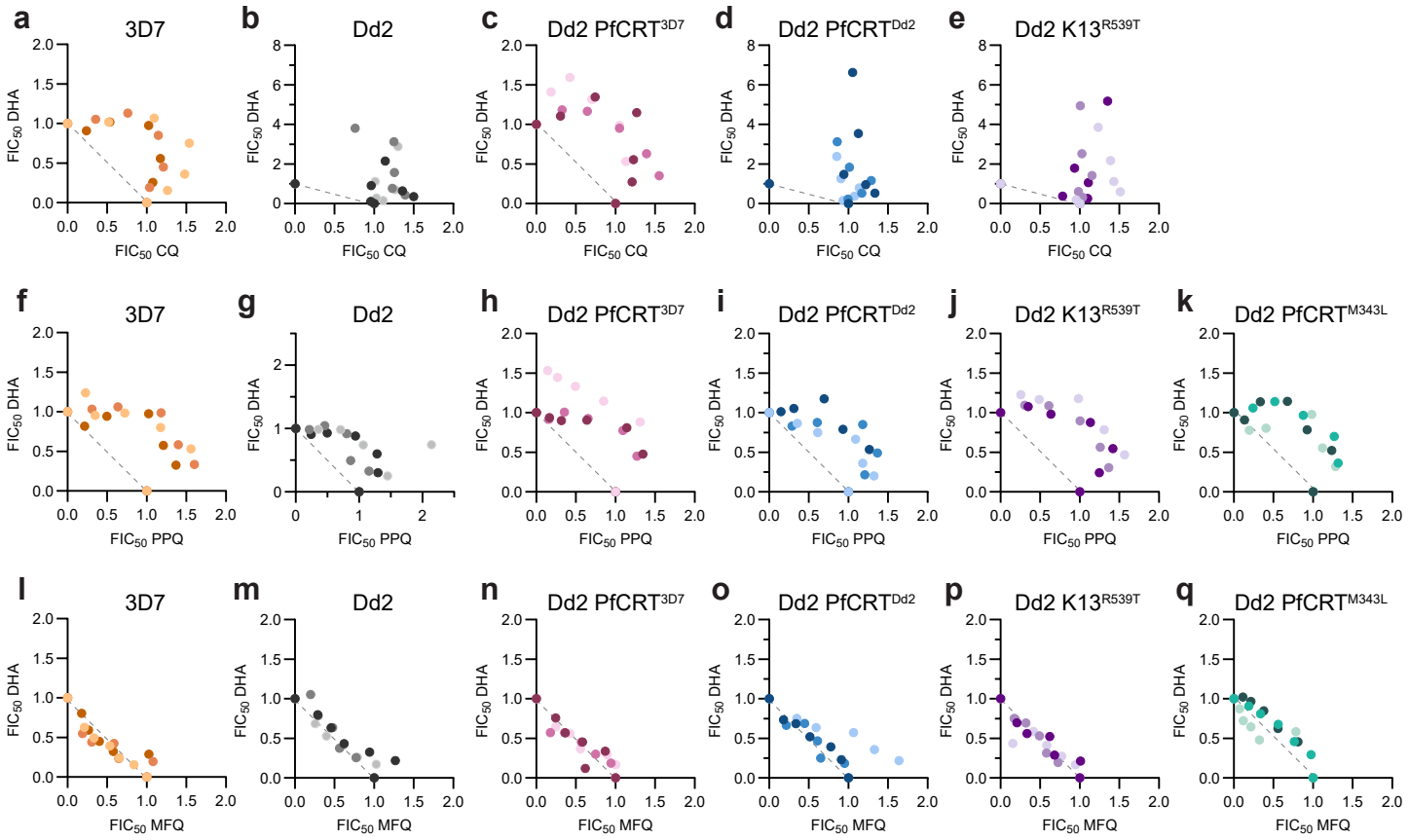

Figure 1. CQ and DHA are superantagonistic in CQ-resistant parasites.
Shown are trophozoite-stage isobolograms for (**a-e**) CQ-DHA, (**f-k**) PPQ-DHA, and (**l-q**) MFQ-DHA. The dotted line on each graph represents perfect additivity. 3D7, Dd2, Dd2 PfCRT^{3D7}, Dd2 PfCRT^{Dd2}, Dd2 K13^{R539T}, and Dd2 PfCRT^{M343L} parasites are indicated in orange, grey, pink, blue, purple, and teal, respectively. Data from three independent replicates are indicated by different shading.

Figure supplement 1. CQ, DHA, PPQ, and MFQ sensitivity of different parasites.

Figure 2

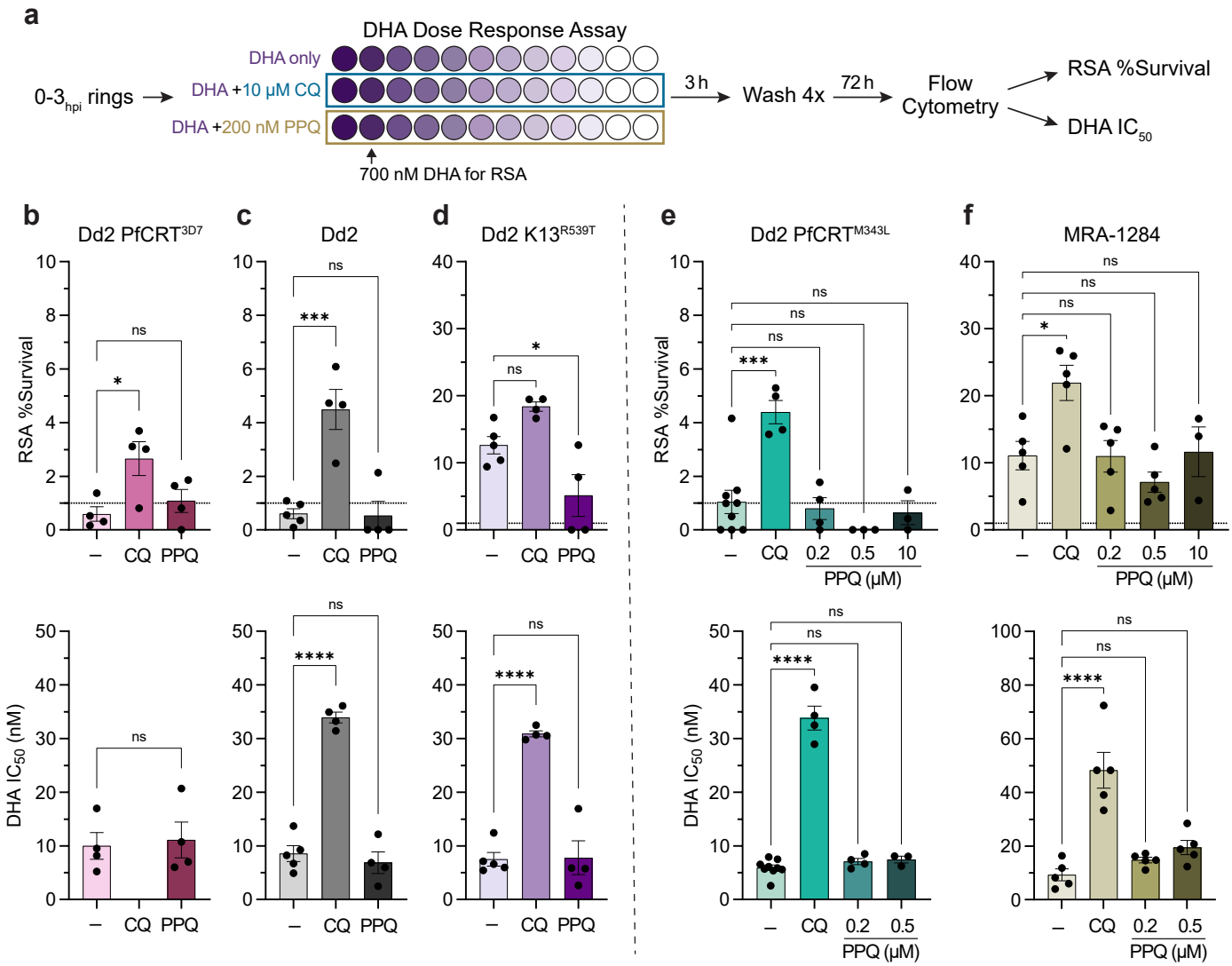

Figure 2. CQ co-treatment confers artemisinin resistance in K13^{WT} parasites.

(**a**) DHA dose response assays were performed on 0-3 hours post invasion (hpi) ring stage parasites. Two-fold serial dilutions of DHA were prepared in 96-well plates (DHA concentration represented by different shades of purple) starting at 1.4 μM so that both IC50 values and RSA survival values at 700 nM DHA could be determined. To evaluate quinoline-DHA interactions in early ring stages, DHA titrations were prepared with fixed concentrations of 10 μM CQ or 200 nM PPQ. (**b-d**) Mean RSA survival values ± SEM (***top panel***) and mean DHA IC50 values ± SEM (***bottom panel***) are shown for (**b**) Dd2 PfCRT^{3D7}, (**c**) Dd2, and (**d**) Dd2 K13^{R539T} parasites. For the PPQ-resistant parasites (**e**) Dd2 PfCRT^{M343L} and (**f**) MRA-1284, additional fixed PPQ concentrations of 500 nM and 10 μM were also tested. For **b** *bottom panel*, a student's t-test was used to assess statistical differences between DHA alone versus DHA + PPQ. For all other graphs, statistical differences between DHA alone (-) and DHA + quinolines was assessed using a one-way ANOVA with a Dunnett's test for multiple comparisons. ****$p < 0.0001$; ***$p < 0.001$; *$p < 0.05$; ns = not significant.

Figure supplement 1. Early ring stage dose-response curves.

Figure 3

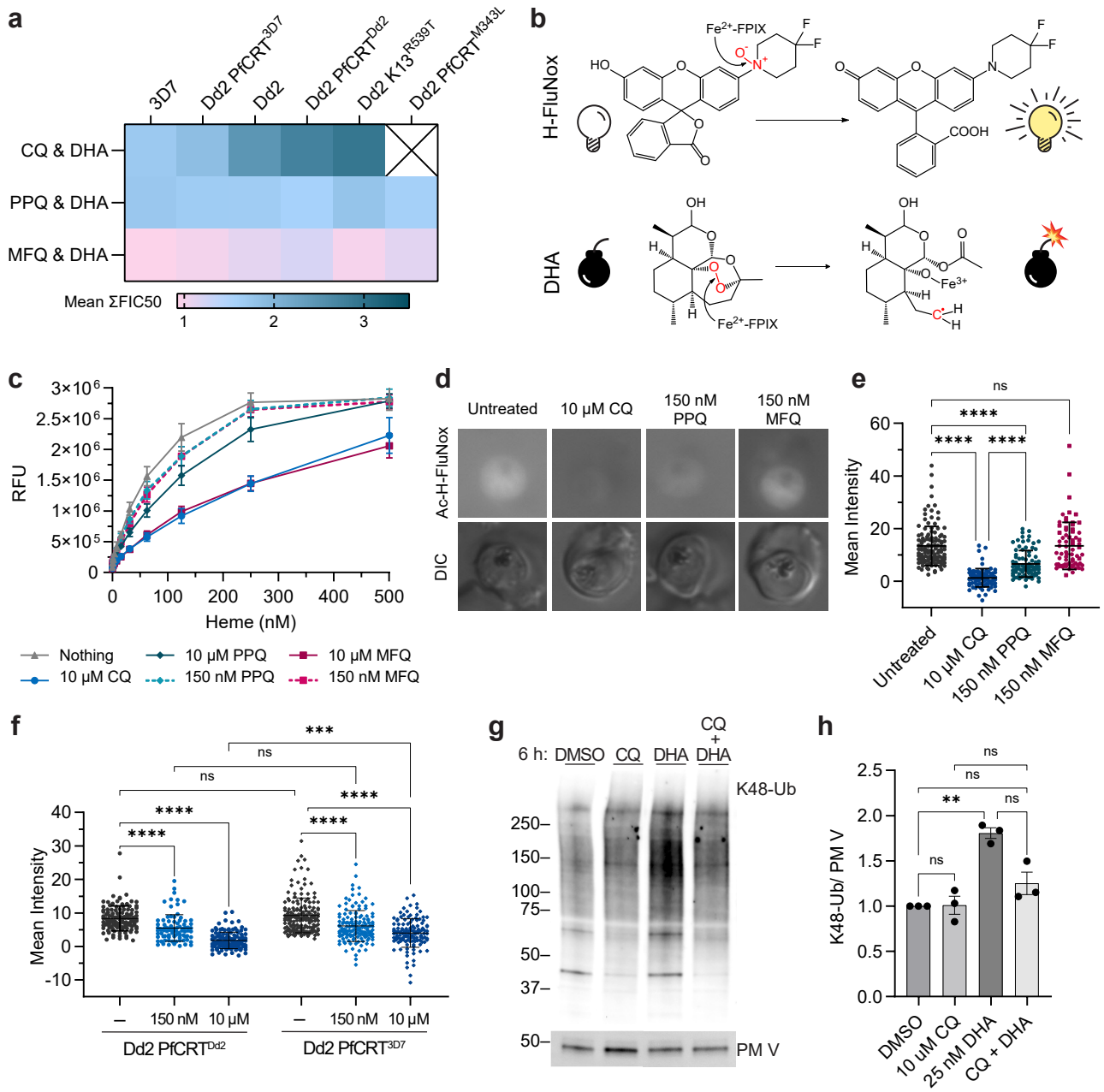
a
3D7
Dd2 PfCRT3D7
Dd2
Dd2 PfCRTDd2
Dd2 K13R539T
Dd2 PfCRTM343L
CQ & DHA
PPQ & DHA
MFQ & DHA
Mean ΣFIC50
1
2
3
b
H-FluNox
DHA
Fe2+-FPIX
COOH
OH
Fe3+
c
RFU
Heme (nM)
Nothing
10 μM CQ
10 μM PPQ
150 nM PPQ
10 μM MFQ
150 nM MFQ
d
Untreated
10 μM CQ
150 nM PPQ
150 nM MFQ
Ac-H-FluNox
DIC
e
Mean Intensity
ns
****
Untreated
10 μM CQ
150 nM PPQ
150 nM MFQ
f
Mean Intensity
***
ns
****
Dd2 PfCRTDd2
Dd2 PfCRT3D7
150 nM
10 μM
g
6 h: DMSO CQ DHA CQ + DHA
K48-Ub
PM V
h
K48-Ub/ PM V
ns
**
DMSO
10 uM CQ
25 nM DHA
CQ + DHA

Figure 3

Figure 3. CQ and PPQ antagonize DHA activation by "inactivating" heme.

(**a**) Shown are mean ΣFIC50 values calculated from the trophozoite stage isobolograms in Figure 1. Values close to 1 (pink) indicate additivity. Values ranging from 1.25 to 2 (light blue) indicate classical antagonism. Values > 2.25 (dark turquoise) indicate superantagonism. (**b *top panel***) Heme (Fe^{2+}-FPIX) cleaves the N-O bond of H-FluNox, mediating probe fluorescence. (**b *bottom panel***) Heme cleaves the peroxide bridge of DHA, which generates a carbon centered radical that can alkylate proximal biomolecules. (**c**) H-FluNox was incubated with increasing concentrations of heme in the presence or absence of 10 μM CQ, 150 nM PPQ, 10 μM PPQ, 150 nM MFQ, or 10 μM MFQ. Shown are mean relative fluorescence units (RFU) ± SD from at least three independent replicates performed in technical triplicate. (**d and e**) Dd2 trophozoites were treated with 10 μM CQ, 150 nM PPQ, 150 nM MFQ, or mock treated for 5.5 h. (**f**) Dd2 $PfCRT^{Dd2}$ and Dd2 $PfCRT^{3D7}$ trophozoites were mock treated or treated with 150 nM CQ or 10 μM CQ for 5.5 h. (**d-f**) Parasites were then incubated with 10 μM Ac-H-FluNox (the cell permeable analog of H-FluNox) to visualize and quantify "active" heme. Shown are (**d**) representative images and (**e and f**) mean fluorescence intensity ± SD of at least 70 parasites from at least three independent drug treatments. Statistical significance was assessed using a one-way ANOVA with a Turkey's test for multiple comparisons. (**g and h**) Dd2 trophozoites were treated with 10 μM CQ, 25 nM DHA, 10 μM CQ + 25 nM DHA for 6 h. Parasite lysates were subjected to western blot and probed with anti-K48-linked ubiquitin (K48-Ub) antibodies or anti-plasmepsin V (PMV) antibodies. Shown is a (**g**) representative blot and (**h**) quantification of relative K48-Ub intensity ± SEM from three independent replicates. Statistical significance between mock treated and antimalarial-treated parasites was determined using a one-way ANOVA with a Turkey's test for multiple comparisons. ****$p < 0.0001$; ***$p < 0.001$; **$p < 0.01$; ns = not significant.

Figure supplement 1. Effect of pH on H-FluNox and Ac-H-FluNox activity.

Figure supplement 2. Equimolar comparison of CQ, PPQ, and MFQ on Ac-H-FluNox fluorescence.

Figure supplement 3. Representative images of Dd2 $PfCRT^{Dd2}$ and Dd2 $PfCRT^{3D7}$ Ac-H-FluNox fluorescence.

Figure supplement 4. Additional K48-ubiquitin western blots.

Table supplement 1. Mean parasite intensity for Ac-H-FluNox experiments.

Source data 1. Uncropped western blots used for ImageJ quantification.

Figure 4

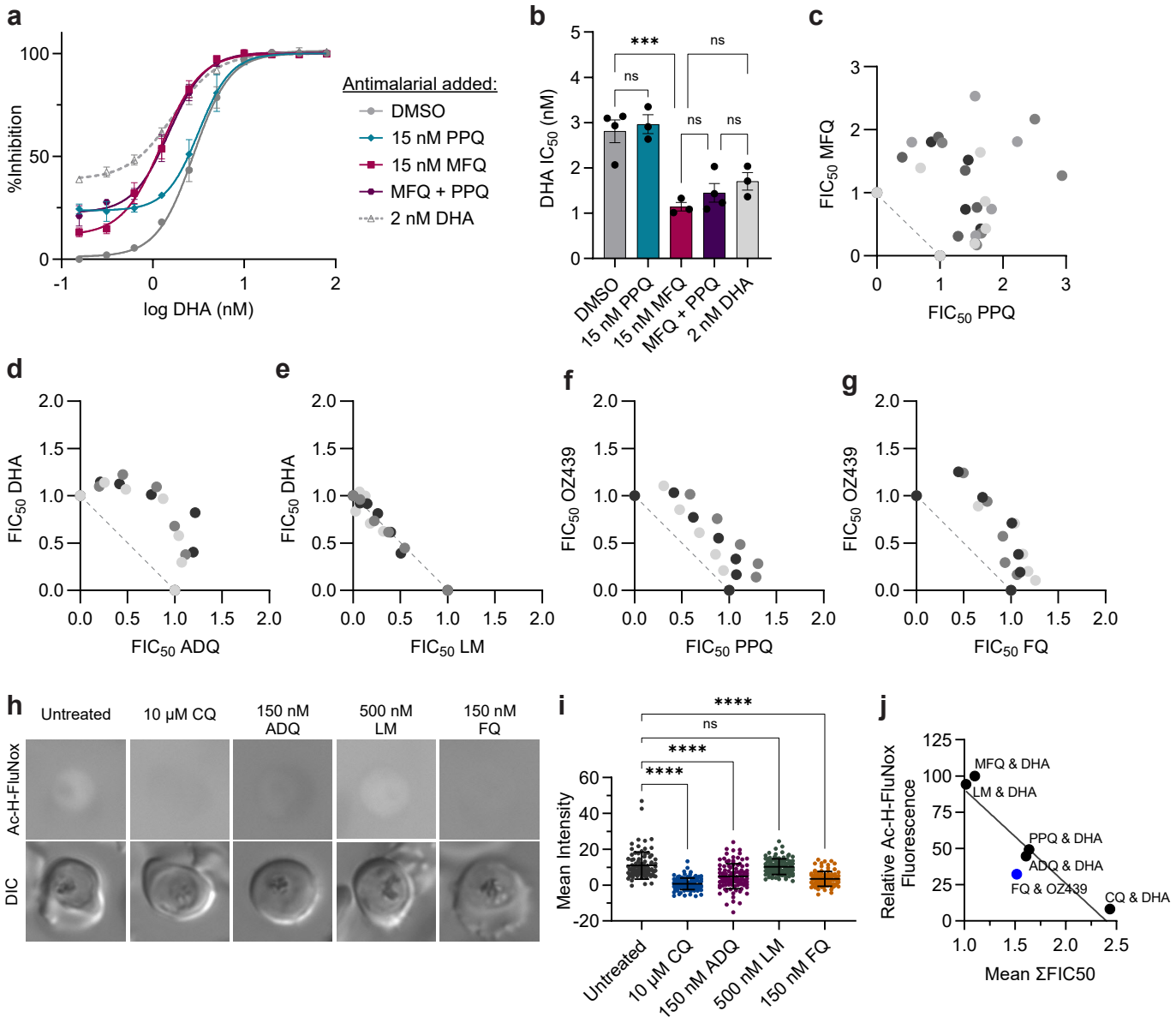
a
%Inhibition
log DHA (nM)
Antimalarial added:
DMSO
15 nM PPQ
15 nM MFQ
MFQ + PPQ
2 nM DHA
b
DHA IC50 (nM)
***
ns
ns
ns
ns
DMSO
15 nM PPQ
15 nM MFQ
MFQ + PPQ
2 nM DHA
c
FIC50 MFQ
FIC50 PPQ
d
FIC50 DHA
FIC50 ADQ
e
FIC50 DHA
FIC50 LM
f
FIC50 OZ439
FIC50 PPQ
g
FIC50 OZ439
FIC50 FQ
h
Untreated
10 μM CQ
150 nM ADQ
500 nM LM
150 nM FQ
Ac-H-FluNox
DIC
i
Mean Intensity
****
ns
****
****
Untreated
10 μM CQ
150 nM ADQ
500 nM LM
150 nM FQ
j
Relative Ac-H-FluNox Fluorescence
Mean ΣFIC50
MFQ & DHA
LM & DHA
PPQ & DHA
ADQ & DHA
FQ & OZ439
CQ & DHA

Figure 4

Figure 4. Quinolines antagonize peroxides. (**a** and **b**) Trophozoite-stage DHA dose-response assays were performed with Dd2 parasites in the presence or absence of 15 nM PPQ, 15 nM MFQ, 15 nM PPQ + 15 nM MFQ, or 2 nM DHA. Shown are (**a**) dose-response curves with mean % inhibition ± SEM and (**b**) mean IC50 values ± SEM from at least three independent replicates. Statistical significance was determined using a one-way ANOVA with a Turkey's test for multiple comparisons. Trophozoite-stage isobolograms were performed on Dd2 parasites to determine drug-drug interactions of (**c**) PPQ-MFQ, (**d**) ADQ-DHA, (**e**) LM-DHA, (**f**) PPQ-OZ439, and (**g**) FQ-OZ439 using the following fixed ratios: 1:0, 4:1, 2:1, 1:1, 1:2, 1:4, 0:1. Shown are fractional IC50 values from at least 3 independent replicates. Independent replicates are indicated in different shading and the diagonal dotted line on each plot indicates perfect additivity. (**h and i**) Dd2 parasites were mock treated or treated with 10 μM CQ, 150 nM ADQ, 500 nM LM, or 150 nM FQ for 5.5 h and free heme was then labeled in live parasites with Ac-H-FluNox. Shown are (**h**) representative images and (**i**) mean fluorescence intensity ± SD of at least 90 parasites from three independent drug treatments. Statistical significance was assessed using a one-way ANOVA with a Dunnett's test for multiple comparisons. ****$p < 0.0001$; ns = not significant. (**j**) Mean relative fluorescence of Ac-H-FluNox from drug treatments in Figure 3e and 4i was plotted against Dd2 mean ΣFIC50 values for the indicated combinations. Combinations with DHA are indicated in black. Combinations with OZ439 are indicated in blue.

Figure supplement 1. Additional MFQ isobolograms.

Figure supplement 2. ADQ, LM, and FQ IC50 values.

Table supplement 1. Mean parasite intensity for Ac-H-FluNox experiments.

Table 1

Parasite Name	Origin	PfCRT Genotype										K13 Genotype	Resistance
		74	75	76	97	220	271	326	343	356	371		
3D7	Africa (1981)	M	N	K	H	A	Q	N	M	I	R	WT	-
Dd2	Indochina (1980)	I	E	T	H	S	E	S	M	T	I	WT	CQ
Dd2 PfCRT^{Dd2}	Edited (introns removed	I	E	T	H	S	E	S	M	T	I	WT	CQ
Dd2 PfCRT^{3D7}	Edited	M	N	K	H	A	Q	N	M	I	R	WT	-
Dd2 K13^{R539T}	Edited	I	E	T	H	S	E	S	M	T	I	R539T	CQ, DHA
Dd2 PfCRT^{M343L}	Edited	I	E	T	H	S	E	S	L	T	I	WT	CQ, PPQ
MRA-1284 (IPC_6261)	Cambodia (2012)	I	E	T	Y	S	E	S	M	T	I	C580Y	DHA, PPQ

Table 1. Parasite strains used in this study. Strains are annotated with their origin (isolate or edited), chloroquine resistance transporter (PfCRT) genotype, Kelch 13 (K13) genotype, and whether they are resistant to CQ, PPQ, or DHA. Wild-type (WT) K13 corresponds to the 3D7 genotype.